

# **Thermal Stability of Dialkylimidazolium Tetrafluoroborate and Hexafluorophosphate Ionic Liquids: *Ex Situ* Bulk Heating to Complement *In Situ* Mass Spectrometry**

Coby J. Clarke<sup>#\*</sup>, Simon Puttick, Thomas J. Sanderson, Alasdair W. Taylor, Richard A. Bourne<sup>§\*</sup>, Kevin R. J. Lovelock<sup>†\*</sup> and Peter Licence

Affiliations:

School of Chemistry, The University of Nottingham, University Park, Nottingham, NG7 2RD, U.K.

\*Current address:

Current Address: <sup>#</sup> Department of Chemical Engineering, Imperial College London, London, UK.

Current Address: <sup>§</sup> Department of Chemistry, University of Leeds, Leeds, UK.

Current Address: <sup>†</sup> Department of Chemistry, University of Reading, Reading, UK.

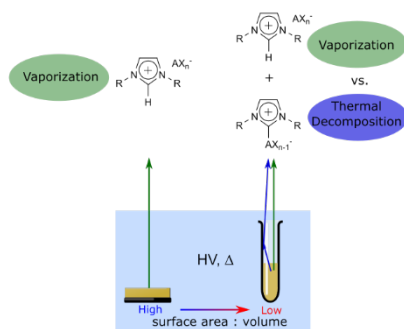
\*Correspondence to:

Coby.clarke@imperial.ac.uk

k.r.j.lovelock@reading.ac.uk

r.a.bourne@leeds.ac.uk

## Graphical Abstract



Competition between vaporization and thermal decomposition of ionic liquids can be influenced by sample mounting during *in situ* measurements.

## Abstract

Thermal decomposition (TD) products of the ionic liquids (ILs)  $[C_nC_1Im][BF_4]$  and  $[C_nC_1Im][PF_6]$  ( $[C_nC_1Im]^+ = 1\text{-alkyl-3-methylimidazolium}$ ,  $[BF_4]^- = \text{tetrafluoroborate}$ , and  $[PF_6]^- = \text{hexafluorophosphate}$ ) were prepared, *ex situ*, by bulk heating experiments in a bespoke setup. The respective products,  $C_nC_1(C_3N_2H_2)BF_3$  and  $C_nC_1(C_3N_2H_2)PF_5$  (1-alkyl-3-methylimidazolium-2-trifluoroborate and 1-alkyl-3-methylimidazolium-2-pentafluorophosphate), were then vaporized and analyzed by direct insertion mass spectrometry (DIMS) in order to identify their characteristic MS signals. During IL DIMS experiments we were subsequently able, *in situ*, to identify and monitor signals due to both IL vaporization and IL thermal decomposition. These decomposition products have not been observed *in situ* during previous analytical vaporization studies of similar ILs. The *ex situ* preparation of TD products is therefore perfectly complementary to *in situ* thermal stability measurements. Experimental parameters such as sample surface area to volume ratios and heating rates are consequently very important for ILs that show competitive vaporization and thermal decomposition. We have explained these experimental factors in terms of Langmuir evaporation and Knudsen effusion-like conditions, allowing us to draw together observations from previous studies to make sense of the literature on IL thermal stability. Hence, the design of experimental setups are crucial and previously overlooked experimental factors.

## 1. Introduction

For many applications of ionic liquids (ILs), low temperature molten salts composed entirely of mobile cations and anions, a pivotal property is thermal stability. Examples of elevated temperature IL processes include catalysis,<sup>1</sup> electrochemical cells,<sup>2</sup> electrodeposition,<sup>2</sup> stationary phases for gas chromatography,<sup>3</sup> lubricants,<sup>4</sup> biomass dissolution,<sup>5</sup> and gas absorption, to name a few.<sup>6</sup> Poor thermal stability can lead to the loss of expensive ILs, and the presence of liquid phase thermal decomposition (TD) products can change the physicochemical properties of the IL solution. Therefore, understanding the thermally driven processes of ILs is key to many of these applications and any future application that operates at elevated temperatures.  $[C_nC_1Im][BF_4]$  and  $[C_nC_1Im][PF_6]$  ILs ( $[C_nC_1Im]^+ = 1\text{-alkyl-3-methylimidazolium}$ ,  $[BF_4]^- = \text{tetrafluoroborate}$ , and  $[PF_6]^- = \text{hexafluorophosphate}$ ) are widely studied in academia, and therefore represent good model ILs for physical property studies. In addition, at the multigram scale the thermolytic conversion of dialkylimidazolium  $[BF_4]^-$  and  $[PF_6]^-$  salts under low to medium vacuum (*i.e.* 25 mbar to  $10^{-3}$  mbar) has become a useful method for the preparation of

substituted imidazol-2-ylidenes, *i.e.* Arduengo carbenes, for use as positron emission tomography probes.<sup>7-11</sup>

Thermal mass loss of ILs can occur by two routes: (i) IL vaporization and (ii) vaporization of liquid phase TD products. Traditionally, these two routes have been treated as separate research fields.<sup>12</sup> For thermogravimetric analysis (TGA) studies of  $[C_nC_1Im][BF_4]$  and  $[C_nC_1Im][PF_6]$ , it was assumed that only TD occurred, and vaporization of the IL was not considered.<sup>13-16</sup> There are four general approaches for studying IL thermal stability:

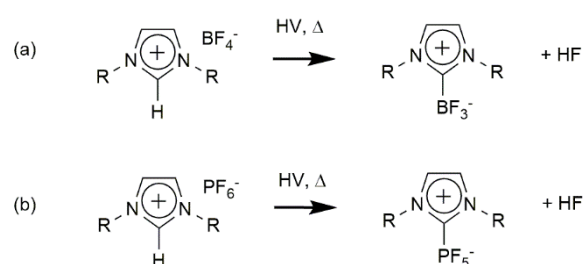
- (i) monitor changes in mass (*e.g.* by quartz crystal microbalance (QCM) or TGA)
- (ii) characterize the condensate of the vapor *ex situ* (*e.g.* using NMR spectroscopy, IR spectroscopy),
- (iii) characterize the residue left after heating the IL *ex situ* (*e.g.* using NMR spectroscopy, IR spectroscopy),
- (iv) identify the vapor *in situ* (*e.g.* using mass spectrometry (MS)).

Approach (i) above can provide temperatures at which mass loss occurs, but gives no information on TD products formed; therefore, competing processes cannot be readily identified. Approaches (ii) and (iii) can be used to identify the mass loss products but tend to give limited information on what occurs at different temperatures. Approach (iv) can potentially give information on both the temperatures at which mass loss occurs and to identify the mass loss products formed.

Using a Knudsen cell at 410 K to 505 K and  $\approx 10^{-5}$  mbar, Zaitsau *et al.* found that  $[C_4C_1Im][PF_6]$  thermally decomposed, with  $E_{a,TD} = 68.0 \pm 2.8$  kJ mol<sup>-1</sup> at  $T = 456.5$  K; no TD products or TD mechanism was given.<sup>17</sup> At  $T > 373$  K, dialkylimidazolium salts with nucleophilic anions (*e.g.*  $[C_nC_1Im][A]$ , where  $[A]^-$  = halide or carboxylate) can thermally decompose by S<sub>N</sub>2 retro-alkylations to give 1-alkylimidazoles ( $C_nIm$ ) and alkylhalides or alkylacetates ( $C_nH_{2n+1}A$ ).<sup>18-26</sup> 1-alkylimidazoles have also been found as TD products for both  $[C_nC_1Im][BF_4]$  and  $[C_nC_1Im][PF_6]$  ILs.<sup>19, 20, 27</sup> For example, MS of the vapor produced when heating  $[C_4C_1Im][PF_6]$  between 425 K to 528 K gave a signal at  $m/z$  96, which was identified as  $[C_2Im]^+$ .<sup>27</sup> It was concluded that the TD product originated from neutral 1-ethylimidazole based upon three pieces of evidence: firstly, the  $m/z$  value of the peak matches that of the parent ion for 1-ethylimidazole; secondly, that the appearance energy for the peak at  $m/z$  96 matched the appearance energy for 1-ethylimidazole (and did not match the appearance energy for  $[C_4C_1Im][PF_6]$  NIPs); thirdly, that no significant  $m/z$  96 peak was observed after electron ionization of the vapor of  $[C_4C_1Im][NTf_2]$  (where  $[NTf_2]^-$  = bis(trifluoromethanesulfonyl)imide). For  $[C_nC_1Im][BF_4]$  ILs, dialkylimidazolium-2-trifluoroborates, *i.e.*  $(CH_3)(C_nH_{2n+1})(C_3N_2H_2)BF_3$  (abbreviated to  $C_nC_1(C_3N_2H_2)BF_3$  in this paper), were found as a TD product (HF is a by-product, see **Scheme 1a**).<sup>28, 29</sup> For  $[C_1C_1Im][PF_6]$  analogous dialkylimidazolium-2-pentafluorophosphates TD products, *i.e.*  $(CH_3)(C_nH_{2n+1})(C_3N_2H_2)PF_5$  (abbreviated to  $C_nC_1(C_3N_2H_2)PF_5$  in this paper), have also been identified (with HF as a by-product, see **Scheme 1b**).<sup>29</sup> For calculations of IL TD, prior knowledge of the liquid phase TD products was required for the methods used to date.<sup>26, 30, 31</sup> Kroon *et al.* used *ab initio* quantum chemical calculations to investigate two different pathways for TD of  $[C_4C_1Im][BF_4]$  and  $[C_4C_1Im][PF_6]$ .<sup>30</sup> For pathway one the TD products were an unstable carbene (1-butyl-3-methylimidazol-2-ylidene), HF and  $BF_3/PF_5$ , and for pathway two the TD products were  $C_4Im$  (1-butylimidazole),  $CH_3F$  and  $BF_3/PF_5$ ; for  $[C_4C_1Im][PF_6]$  the activation energies of TD ( $E_{a,TD}$ ) were 313 kJ mol<sup>-1</sup> and 213 kJ mol<sup>-1</sup> for pathways one and two respectively.

Until the mid-2000s, ILs were thought to be involatile; their high enthalpies of vaporization ( $\Delta_{\text{vap}}H$ ) were thought to prevent vaporization before TD occurred. In 2006 Earle *et al.* used a Kugelrohr setup at  $473 \text{ K} < T < 573 \text{ K}$  and pressure  $< 8 \text{ mbar}$  to demonstrate that a range of ILs with different anion and cation combinations could be distilled (*i.e.* physical transfer by vaporization of IL).<sup>32</sup>  $[\text{C}_4\text{C}_1\text{Im}][\text{PF}_6]$  was noted to distil at  $573 \text{ K}$  and  $6 \text{ mbar}$ , without significant TD of the condensate or the residue.<sup>32</sup> A large number of studies have subsequently focused on investigating IL vaporization, most utilizing ILs containing the thermally robust  $[\text{NTf}_2]^-$  anion.<sup>33</sup> Mass spectrometry (MS)<sup>22, 27, 34-55</sup> and simulations<sup>44, 56-59</sup> have since identified the vapor phase of ILs to be composed primarily of neutral ion pairs (NIPs), including for both  $[\text{C}_n\text{C}_1\text{Im}][\text{BF}_4]$  and  $[\text{C}_n\text{C}_1\text{Im}][\text{PF}_6]$  ( $n = 2, 4, 8$ ).<sup>34, 36, 39, 40, 42</sup> Using temperature programmed desorption (TPD) line-of-sight mass spectrometry (LOSMS) only IL NIP vaporization was observed; no evidence was found for the TD of  $[\text{C}_n\text{C}_1\text{Im}][\text{BF}_4]$  to  $\text{C}_n\text{C}_1(\text{C}_3\text{N}_2\text{H}_2)\text{BF}_3$  or  $[\text{C}_n\text{C}_1\text{Im}][\text{PF}_6]$  to  $\text{C}_n\text{C}_1(\text{C}_3\text{N}_2\text{H}_2)\text{PF}_5$  between  $450 \text{ K}$  to  $565 \text{ K}$ .<sup>34, 36, 39, 40</sup> Note that other studies where IL NIP vaporization was detected for  $[\text{C}_n\text{C}_1\text{Im}][\text{BF}_4]$  to or  $[\text{C}_n\text{C}_1\text{Im}][\text{PF}_6]$  did not report  $\text{C}_n\text{C}_1(\text{C}_3\text{N}_2\text{H}_2)\text{BF}_3$  or  $\text{C}_n\text{C}_1(\text{C}_3\text{N}_2\text{H}_2)\text{PF}_5$  formation.<sup>27, 42</sup> Furthermore, IR spectroscopy of the condensate and residue from quartz-crystal microbalance (QCM) measurements of  $[\text{C}_n\text{C}_1\text{Im}][\text{BF}_4]$  and  $[\text{C}_n\text{C}_1\text{Im}][\text{PF}_6]$  ( $n = 2, 4, 6, 8, 10$ ) between  $403 \text{ K}$  to  $461 \text{ K}$  suggest that these ILs do not thermally decompose under these conditions.<sup>60, 61</sup>

Recently, it has been appreciated that understanding the competition between the two possible routes for IL mass loss, IL vaporization and TD product vaporization, is key for understanding thermal mass loss of IL.<sup>22, 27, 62-65</sup> However, the literature for dialkylimidazolium  $[\text{BF}_4]^-$  and  $[\text{PF}_6]^-$  ILs appears to be contradictory; it is unclear under what conditions vaporization or TD will occur. For example, the condensate collected after heating  $[\text{C}_n\text{C}_1\text{Im}][\text{BF}_4]$  ILs under high vacuum ( $10^{-3}$  to  $10^{-5} \text{ mbar}$ ) and  $T > 523 \text{ K}$  gave mixtures of IL distillate and the TD product  $\text{C}_n\text{C}_1(\text{C}_3\text{N}_2\text{H}_2)\text{BF}_3$ .<sup>28</sup> By monitoring mass loss between  $453 \text{ K}$  to  $551 \text{ K}$ , Volpe *et al.* found competition between TD product vaporization and IL vaporization for  $[\text{C}_4\text{C}_1\text{Im}][\text{PF}_6]$  by altering the orifice size of a Knudsen effusion cell.<sup>27</sup> However, many other studies have reported either TD<sup>13-17, 19, 20</sup> or IL vaporization<sup>34, 36, 39, 40, 42, 60, 61, 66</sup>.

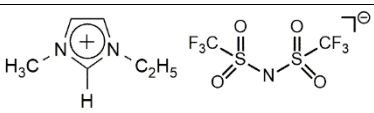
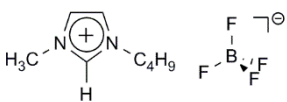
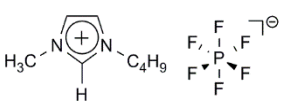
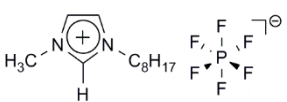


**Scheme 1** The thermal decomposition (TD) of ionic liquids (ILs) under high vacuum (HV): (a) dialkylimidazolium tetrafluoroborate to form dialkylimidazolium-2-trifluoroborate and HF, (b) dialkylimidazolium hexafluorophosphate to form dialkylimidazolium-2-pentafluorophosphate and HF.

In this paper, we present data on the condensation products of bulk heating experiments and direct insertion mass spectrometry (DIMS) results for  $[\text{C}_4\text{C}_1\text{Im}][\text{BF}_4]$  and  $[\text{C}_n\text{C}_1\text{Im}][\text{PF}_6]$  (where  $n = 4, 8$ ) that show how *ex situ* preparation enables a TD product to be definitively identified during *in situ* MS experiments. We therefore exploit a combination of approaches (*i.e.* ii-iv from the introduction list) by characterising (using *ex situ* characterization techniques) the condensates from bulk heating experiments and we identify, using *in situ* MS, the vapor produced by heating the same ILs. Our experiments demonstrate that previous studies aimed at understanding the TD of dialkylimidazolium

$[\text{BF}_4]^-$  and  $[\text{PF}_6]^-$  ILs may have been restricted by upper mass limits. The abbreviations, structures, names, and molar mass for ILs investigated in this work are given in **Table 1**.

**Table 1** Summary of the ionic liquids investigated in this study. The molar masses are calculated using the most intense isotope for all elements. Note:  $[\text{C}_2\text{C}_1\text{Im}][\text{NTf}_2]$  was used as a thermally robust comparison for bulk heating experiments (see the ESI).

Abbreviation	Structure	Name	Cation $M / \text{g mol}^{-1}$	Anion $M / \text{g mol}^{-1}$
$[\text{C}_2\text{C}_1\text{Im}][\text{NTf}_2]$		1-ethyl-3-methylimidazolium bis(trifluoromethanesulfonyl)imide	111	280
$[\text{C}_4\text{C}_1\text{Im}][\text{BF}_4]$		1-butyl-3-methylimidazolium tetrafluoroborate	139	87
$[\text{C}_4\text{C}_1\text{Im}][\text{PF}_6]$		1-butyl-3-methylimidazolium hexafluorophosphate	139	145
$[\text{C}_8\text{C}_1\text{Im}][\text{PF}_6]$		1-octyl-3-methylimidazolium hexafluorophosphate	195	145

## 2. Experimental

### 2.1 Ionic Liquid Synthesis

Synthetic procedures of the ILs used in this work are reported in the Supplementary Information. All ILs were degassed for 24 h on a Schlenk line ( $p \approx 5 \times 10^{-2}$  mbar,  $T = 313$  K) prior to transferring to the condensation apparatus. It must be noted that the presence of water can lead to hydrolysis of  $[C_nC_1Im][BF_4]$  and  $[C_nC_1Im][PF_6]$  ILs.<sup>67</sup> However,  $^{19}F$  NMR showed no evidence of additional components, resulting from hydrolysis, prior to condensation or MS experiments.

### 2.2 Vaporization + condensation apparatus and method

Vaporization + condensation experiments were carried out using a custom designed glass condensation apparatus evacuated using a diffusion pump. The setup was developed to increase IL vaporization rates compared to the previous vaporization + condensation apparatus employed by our group.<sup>28, 38</sup> Briefly, a blown glass still pot with integrated still head and receiver (see **Figure 1**) was filled with the IL of interest and connected to the high vacuum pumping system by way of a standard glass-to-metal seal. Pressure was monitored using a Penning gauge situated on the diffusion pump and a Pirani gauge situated between the condensation apparatus and diffusion pump. The base pressure in the apparatus prior to charging with IL was  $7.5 \times 10^{-6}$  mbar. The still pot was heated by an electrical heating tape that was wrapped around the apparatus, a Type K thermocouple provided temperature measurement. The still pot was insulated with glass wool to maintain a relatively uniform temperature (further details are available in the ESI). The surface area-to-volume ratio was calculated to be 0.0085 for 40 mL of IL in the condensation apparatus.

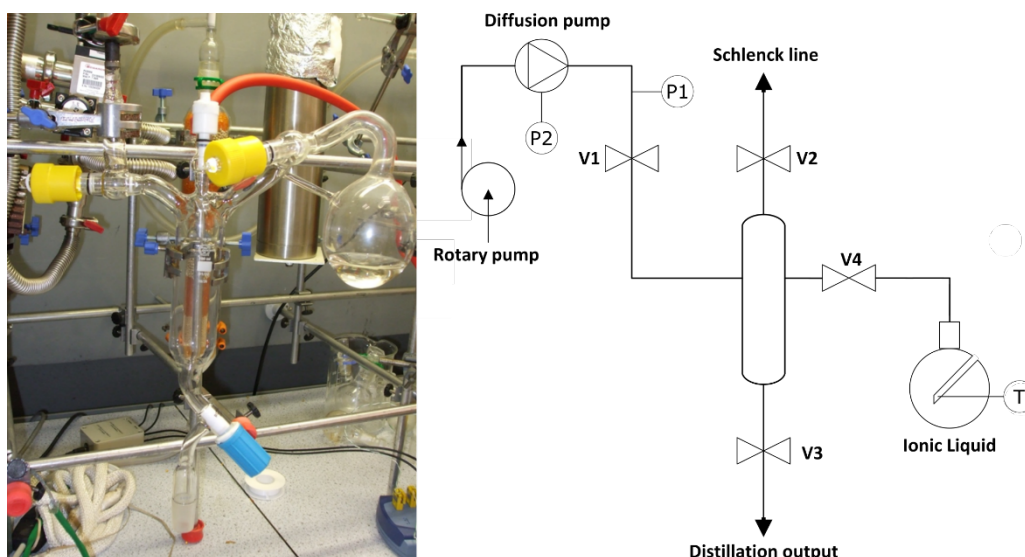


**Figure 1** The condensation apparatus (containing 20 ml ionic liquid) and corresponding process diagram showing the thermocouple (T), Pirani (P1) and Penning gauge (P2) positions.

#### 2.2.1 Ex situ characterization of TD products

For IL heating/condensation experiments,  $^1\text{H}$ ,  $^{13}\text{C}$ ,  $^{19}\text{F}$  and  $^{31}\text{P}$  NMR spectra were recorded at room temperature on either a Bruker DPX300 (300 MHz), Bruker AV400 (400 MHz), or Bruker AV3500 (500 MHz). All NMR spectroscopy samples were prepared in DMSO- $d_6$  and spectra were referenced to the residual solvent signal of DMSO ( $^1\text{H}$  NMR 2.50 ppm,  $^{13}\text{C}$  NMR 39.52 ppm). Electrospray ionization mass spectrometry (ESI-MS) was recorded on a Bruker Micro-TOF mass spectrometer possessing both positive and negative ionization sources. Solutions were made up in analytical reagent grade methanol. The thermally robust ionic liquid 1-ethyl-3-methylimidazolium bis(trifluoromethanesulfonyl)imide,  $[\text{C}_2\text{C}_1\text{Im}][\text{NTf}_2]$ , was used to test the condensation apparatus before investigating other ILs. Bulk vaporization was carried out at 579 K and  $1.1 \times 10^{-5}$  mbar to yield a colorless distillate ( $1.86 \text{ g hr}^{-1}$ ). The  $^1\text{H}$  NMR of the condensate showed that pure IL had been collected and no decomposition had occurred (**Figure S1**). The NMR spectra of  $\text{C}_4\text{C}_1(\text{C}_3\text{N}_2\text{H}_2)\text{PF}_5$  are displayed in the supplementary information (**Figure S2-5**) to show the coupling and multiplicity of the TD products.

#### **$\text{C}_4\text{C}_1(\text{C}_3\text{N}_2\text{H}_2)\text{BF}_3$ from $[\text{C}_4\text{C}_1\text{Im}][\text{BF}_4]$**

$[\text{C}_4\text{C}_1\text{Im}][\text{BF}_4]$  (40 ml, 0.21 mol) was placed into the degassed and dried condensation apparatus *via* a glass syringe under a positive pressure of argon. The system was evacuated using a rotary pump ( $< 5.0 \times 10^{-2}$  mbar), before being opened to the main diffusion pump. After allowing the pressure to equilibrate, the sample was heated to 359 K, causing the pressure to rise to  $4.0 \times 10^{-4}$  mbar. Further heating overnight allowed the base pressure to establish ( $7.2 \times 10^{-6}$  mbar) at this temperature which ensured the removal of any residual volatile impurities. The temperature was raised and a dark orange condensate was observed to condense on the walls of the apparatus at 578 K. Bulk vaporization + condensation occurred at 613 K and  $2 \times 10^{-3}$  mbar to  $4 \times 10^{-3}$  mbar to yield a pale orange liquid condensate ( $9.85 \text{ g}$ ,  $0.37 \text{ g h}^{-1}$ ). For DIMS experiments and to confirm the identity of the condensate, a small portion of the liquid was washed with excess water to remove residual IL.  $^1\text{H}$  NMR (DMSO- $d_6$ , 300 MHz):  $\delta$  7.53 (d,  $J = 1.8 \text{ Hz}$ , 1H), 7.46 (d,  $J = 1.8 \text{ Hz}$ , 1H), 4.16 (t,  $J = 7.6 \text{ Hz}$ , 2H), 3.79 (s, 3H), 1.57-1.82 (m, 2H), 4.09 (d,  $J = 15.0 \text{ Hz}$ , 2H), 0.88 (t,  $J = 7.5 \text{ Hz}$ , 3H).  $^{13}\text{C}$  NMR (DMSO- $d_6$ , 75 MHz):  $\delta$  = 123.0, 121.5, 48.0, 35.7, 32.6, 19.0, 13.4. ESI-MS (MeOH): (+ve) 229.1095 ( $\text{M}+\text{Na}$ ) $^+$ . Data consistent with previous reports.<sup>28</sup>

#### **C<sub>4</sub>C<sub>1</sub>(C<sub>3</sub>N<sub>2</sub>H<sub>2</sub>)PF<sub>5</sub> from [C<sub>4</sub>C<sub>1</sub>Im][PF<sub>6</sub>]**

The same loading and degassing procedure used for [C<sub>4</sub>C<sub>1</sub>Im][BF<sub>4</sub>] was also used for [C<sub>4</sub>C<sub>1</sub>Im][PF<sub>6</sub>]. The bulk vaporization + condensation took place at 641 K and  $1.4 \times 10^{-4}$  mbar to yield a pale orange condensate that solidified upon collecting in a round bottom flask (15.2 g,  $0.66 \text{ g h}^{-1}$ ). For DIMS experiments and to confirm the identity of the condensate, a small portion of the solidified material was recrystallized from methanol/water to give fine white needles that were dried at  $\approx 10^{-2}$  mbar and 323 K. <sup>1</sup>H NMR (400 MHz, DMSO-d<sub>6</sub>)  $\delta$  7.65 (dd,  $J = 3.3, 2.0$  Hz, 1H), 7.58 (dd,  $J = 3.0, 2.0$  Hz, 1H), 4.27 – 4.23 (m, 2H), 3.86 (s, 3H), 1.80 – 1.61 (m, 2H), 1.41 – 1.18 (m, 2H), 0.90 (t,  $J = 7.4$  Hz, 3H). <sup>13</sup>C NMR (126 MHz, DMSO-d<sub>6</sub>)  $\delta$  152.91 (dquin,  $J = 330.6, 62.7$  Hz, 1C), 123.84 (br d,  $J = 9.1$  Hz, 1C), 121.52 (br d,  $J = 10.0$  Hz, 1C), 49.22 (t,  $J = 3.2$  Hz, 1C), 37.70, 32.42, 19.24, 13.46. <sup>19</sup>F NMR (DMSO-d<sub>6</sub>, 377 MHz): Shift = -52.25 (dd,  $J = 782.0, 51.0$  Hz, 4F), -70.60 ppm (dquin,  $J = 755.0, 51.0$  Hz, 1F). <sup>31</sup>P NMR (DMSO-d<sub>6</sub>, 162 MHz):  $\delta$  = -150.65 ppm (dquin,  $J = 781.9, 755.1$  Hz, 1P). ESI-MS (MeOH): (+ve) 287.0705 (M+Na)<sup>+</sup>. Anal. Calcd for C<sub>8</sub>H<sub>14</sub>F<sub>5</sub>N<sub>2</sub>P: C, 36.37; H, 5.34; N, 10.60. Found: C, 36.51; H, 5.32; N, 10.26. HRMS (ESI/QTOF) m/z: [M + Na]<sup>+</sup> Calcd for C<sub>8</sub>H<sub>14</sub>F<sub>5</sub>N<sub>2</sub>NaP<sup>+</sup> 287.0707; Found 287.0705.

#### **C<sub>8</sub>C<sub>1</sub>(C<sub>3</sub>N<sub>2</sub>H<sub>2</sub>)PF<sub>5</sub> from [C<sub>8</sub>C<sub>1</sub>Im][PF<sub>6</sub>]**

The same loading and degassing procedure used for [C<sub>4</sub>C<sub>1</sub>Im][BF<sub>4</sub>] was also used for [C<sub>8</sub>C<sub>1</sub>Im][PF<sub>6</sub>]. The bulk vaporization + condensation took place at 625 K and  $3.7 \times 10^{-4}$  mbar to yield a dark orange liquid condensate (11.7 g,  $0.51 \text{ g h}^{-1}$ ). To confirm the identity of the condensate, a small portion of the liquid was purified by column chromatography (silica gel; DCM) to give a white solid that was dried at  $\approx 10^{-2}$  mbar and 323 K. <sup>1</sup>H NMR (400 MHz, DMSO-d<sub>6</sub>)  $\delta$  7.65 (dd,  $J = 3.2, 2.0$  Hz, 1H), 7.58 (dd,  $J = 3.1, 1.9$  Hz, 1H), 4.26 – 4.21 (m, 2H), 3.86 (s, 3H), 1.76 – 1.68 (m, 2H), 1.31 – 1.21 (m, 10H), 0.85 (t,  $J = 7.0$  Hz, 3H). <sup>13</sup>C NMR (126 MHz, DMSO-d<sub>6</sub>)  $\delta$  152.90 (dquin,  $J = 331.5, 63.1$  Hz, 1C), 123.80 (d,  $J = 10.0$  Hz, 1C), 121.49 (d,  $J = 9.1$  Hz, 1C), 49.43, 37.68, 31.20, 30.40, 28.54, 28.51, 25.92, 22.09, 13.92. <sup>19</sup>F NMR (376 MHz, DMSO-d<sub>6</sub>)  $\delta$  -52.31 (dd,  $J = 781.9, 51.1$  Hz, 4F), -70.66 (dquin,  $J = 754.9, 51.1$  Hz, 1F). <sup>31</sup>P NMR (DMSO-d<sub>6</sub>, 162 MHz):  $\delta$  = -150.63 ppm (dquin,  $J = 781.9, 755.1$  Hz, 1P). HRMS (ESI/QTOF) m/z: [M + Na]<sup>+</sup> Calcd for C<sub>12</sub>H<sub>22</sub>F<sub>5</sub>N<sub>2</sub>NaP<sup>+</sup> 343.1333; Found 343.1316.

### **2.3 Direct insertion mass spectrometry (DIMS)**

Direct insertion mass spectrometry (DIMS) was performed on a Thermo Finnigan PolarisQ ion trap mass spectrometer (with  $\approx 2.5 \times 10^{-6}$  mbar base pressure). ILs were dried on a Schlenk line for 24 h ( $p \approx 5 \times 10^{-2}$  mbar,  $T = 313$  K) before 1 to 2 drops were deposited onto a glass capillary in open air. The capillary was mounted on the direct insertion probe, which was introduced to the spectrometer straight away to limit absorption of water from the air. After equilibrating at 313 K, all ILs were heated by  $10 \text{ K min}^{-1}$  to 623 K, or until sufficient amounts of desorption were observed. Samples were ionized by electron impact ionization (70 eV), and the ion detector was switched from positive to negative detection mode every minute during acquisition. The surface area-to-volume ration for the glass sample holder was calculated to be 0.036, a value far larger than the bulk heating apparatus.

## **3. Results**

### **3.1 Heating bulk [C<sub>4</sub>C<sub>1</sub>Im][BF<sub>4</sub>] followed by *ex situ* characterization of the condensate**



Bulk  $[\text{C}_4\text{C}_1\text{Im}][\text{BF}_4]$  was heated in the vaporization + condensation setup at different temperatures between 543 K and 690 K and the condensates were characterized by NMR spectroscopy. Two different products were obtained,  $[\text{C}_4\text{C}_1\text{Im}][\text{BF}_4]$  and  $\text{C}_4\text{C}_1(\text{C}_3\text{N}_2\text{H}_2)\text{BF}_3$  (**Scheme 2**, parts 1b and 2a-b). The  $^1\text{H}$  NMR spectra show  $\text{C}^4\text{-H}$  and  $\text{C}^5\text{-H}$  protons for  $\text{C}_4\text{C}_1(\text{C}_3\text{N}_2\text{H}_2)\text{BF}_3$  (7.46 and 7.52 ppm) which are shifted upfield of the  $[\text{C}_4\text{C}_1\text{Im}][\text{BF}_4]$   $\text{C}^4\text{-H}$  and  $\text{C}^5\text{-H}$  protons (7.75 and 7.69 ppm) by  $\sim 0.23$  ppm (**Figure 2**). All other protons in both  $[\text{C}_4\text{C}_1\text{Im}][\text{BF}_4]$  and  $\text{C}_4\text{C}_1(\text{C}_3\text{N}_2\text{H}_2)\text{BF}_3$  give similar chemical shifts, apart from the  $\text{C}^2\text{-H}$  signal which is not present in  $\text{C}_4\text{C}_1(\text{C}_3\text{N}_2\text{H}_2)\text{BF}_3$  and therefore not observed in the  $^1\text{H}$  NMR (see **Figure S7**). Integration of the  $\text{C}^4\text{-H}$  and  $\text{C}^5\text{-H}$  signals gave the relative amounts of  $[\text{C}_4\text{C}_1\text{Im}][\text{BF}_4]$  and  $\text{C}_4\text{C}_1(\text{C}_3\text{N}_2\text{H}_2)\text{BF}_3$  in the condensates. **Figure 3** shows the composition of condensates collected from seven separate bulk scale attempts at the distillation of  $[\text{C}_4\text{C}_1\text{Im}][\text{BF}_4]$  at different  $T$  between 543 K and 690 K. At  $T < 583$  K, IL distillation and production of  $\text{C}_4\text{C}_1(\text{C}_3\text{N}_2\text{H}_2)\text{BF}_3$  occur as competing processes, *e.g.* at 543 K the ratio of  $[\text{C}_4\text{C}_1\text{Im}][\text{BF}_4] : \text{C}_4\text{C}_1(\text{C}_3\text{N}_2\text{H}_2)\text{BF}_3$  was 37:63. However, at  $T > 583$  K the amount of distilled  $[\text{C}_4\text{C}_1\text{Im}][\text{BF}_4]$  decreases, giving  $\text{C}_4\text{C}_1(\text{C}_3\text{N}_2\text{H}_2)\text{BF}_3$  as the major product, *e.g.* at 690 K the ratio was 7:93. An optimized yield of 95% was achieved at 623 K in the vaporization + condensation setup.

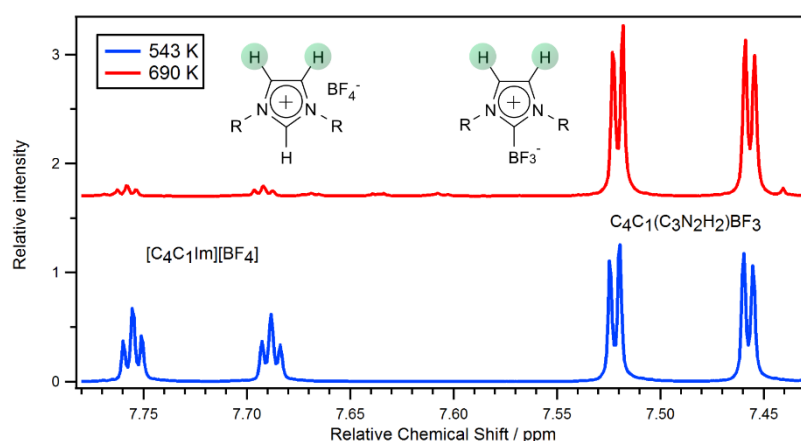


**Figure 2** The  $\text{C}^4\text{-H}$  and  $\text{C}^5\text{-H}$  protons of  $[\text{C}_4\text{C}_1\text{Im}][\text{BF}_4]$  and  $\text{C}_4\text{C}_1(\text{C}_3\text{N}_2\text{H}_2)\text{BF}_3$  (highlighted in green) in the  $^1\text{H}$  NMR spectroscopy of the condensates from  $[\text{C}_4\text{C}_1\text{Im}][\text{BF}_4]$  vaporization + condensation experiments at 543 K and 690 K.

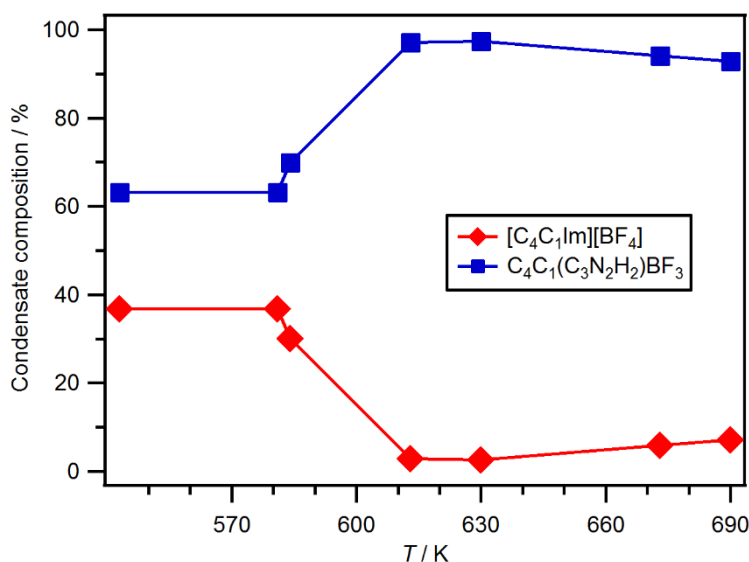


**Figure 3** The composition of the condensate for bulk scale vaporization + condensation experiments for  $[C_4C_1Im][BF_4]$  at different  $T$  between 543 K and 690 K, as determined by  $^1H$  NMR spectroscopy.

### 3.2 Heating thin films of $C_4C_1(C_3N_2H_2)BF_3$ : *in situ* mass spectrometry of the vapor phase

To understand the MS of  $[C_4C_1Im][BF_4]$ , it is necessary to first investigate  $C_4C_1(C_3N_2H_2)BF_3$  using MS. There are two parts to studying the MS of  $C_4C_1(C_3N_2H_2)BF_3$ , firstly identifying the vapor phase composition and secondly determining at what temperatures vaporization occurs. Summaries of the key fragment cations and anions are given in **Table 2** and **Table 3** respectively. At 323 K in positive mode for  $C_4C_1(C_3N_2H_2)BF_3$ , **Figure 4a**, the peak at  $m/z$  187 is  $C_4C_1(C_3N_2H_2)BF_3$  minus one fluorine,  $[C_4C_1(C_3N_2H_2)^{11}BF_2]^+$  (**Scheme 2**, step 2c(ii)). A peak at  $m/z$  186, approximately four times lower intensity than the  $m/z$  187 peak, is  $[C_4C_1(C_3N_2H_2)^{10}BF_2]^+$ , an isotopic cation. No peak due to the  $C_4C_1(C_3N_2H_2)BF_3$  molecular ion,  $[C_4C_1(C_3N_2H_2)BF_3]^+$ , was observed at  $m/z$  206 (**Scheme 2**, step 2c(i)). The peaks at  $m/z$  137,  $m/z$  95 and  $m/z$  82 are all cationic fragments of the  $[C_4C_1Im]^+$  parent.<sup>39</sup> At higher temperatures, *e.g.* 391 K, a peak at  $m/z$  393 was observed in the positive mode mass spectrum for  $C_4C_1(C_3N_2H_2)BF_3$ , indicating formation of dimers (i.e.  $[C_4H_9CH_3(C_3N_2H_2)BF_2(C_4C_1(C_3N_2H_2)BF_3)]^+$ ) in the vapor phase (**Figure S8**). For the negative mode mass spectra, three peaks were observed between 323 K and 391 K; an example mass spectrum is given in **Figure 4b** at 368 K. The  $m/z$  205 peak is  $C_4C_1(C_3N_2H_2)BF_3$  minus one hydrogen. It is unclear whether loss of this hydrogen occurred from an alkyl group or from the ring; the fragment anion is labelled as  $[C_4C_1(C_3N_2H)^{11}BF_3]^-$ , corresponding to loss of one hydrogen from the ring. The  $m/z$  149 peak is due to  $[C_1(C_3N_2H_2)^{11}BF_3]^-$  and the  $m/z$  81 peak is due to  $[C_1(C_3N_2H_2)]^-$ . Therefore, all evidence points to vaporization of intact  $C_4C_1(C_3N_2H_2)BF_3$ .

The intensities of the peaks recorded in negative mode MS were significantly lower than those recorded in positive mode MS for the vapor of  $C_4C_1(C_3N_2H_2)BF_3$ . This significant difference is somewhat masked by the negative mode mass spectrum (**Figure 4b**) being recorded at 45 K higher temperature than the positive mode mass spectrum (**Figure 4a**); at 323 K the signal-to-noise ratio was very poor. A relatively intense  $m/z$  96 peak was observed for positive mode DIMS of  $C_4C_1(C_3N_2H_2)BF_3$  (**Figure 4a**). Therefore, this  $m/z$  96 peak was a fragmentation product of  $C_4C_1(C_3N_2H_2)BF_3$ .

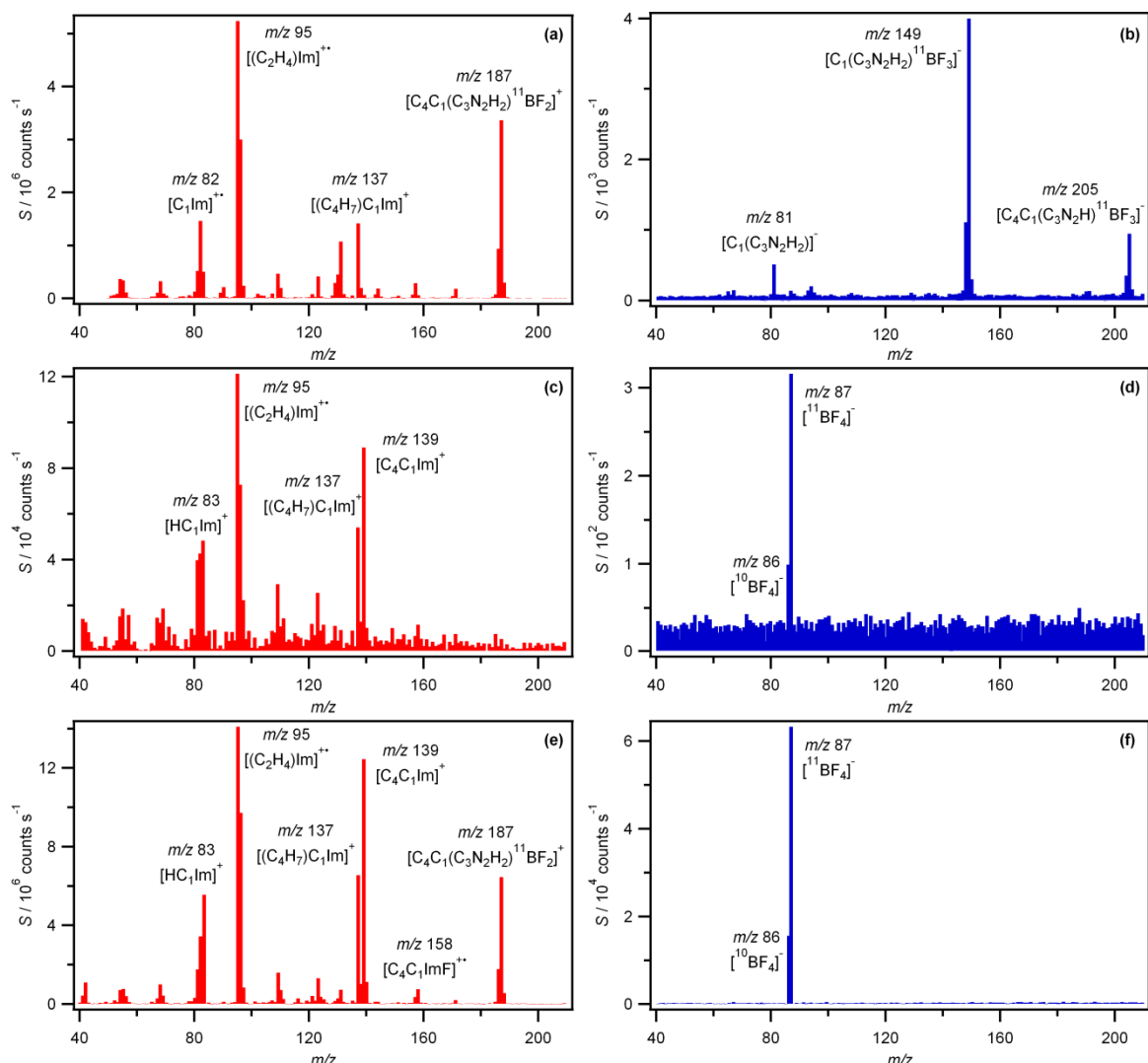


**Figure 4** Mass spectrum intensity versus  $m/z$  for: (a)  $C_4C_1(C_3N_2H_2)BF_3$  in positive mode at 323 K, (b)  $C_4C_1(C_3N_2H_2)BF_3$  in negative mode at 368 K, (c)  $[C_4C_1Im][BF_4]$  in positive mode at 500 K, (d)  $[C_4C_1Im][BF_4]$  in negative mode at 500 K, (e)  $[C_4C_1Im][BF_4]$  in positive mode at 640 K, (f)  $[C_4C_1Im][BF_4]$  in negative mode at 640 K.

The peak at  $m/z$  187 was used to monitor  $C_4C_1(C_3N_2H_2)BF_3$  vaporization with respect to  $T$  (**Figure 5a**). Vaporization of  $C_4C_1(C_3N_2H_2)BF_3$  occurs significantly at 323 K, and is complete by  $\sim 400$  K. For this mass spectrometer, the lowest starting  $T$  for experiments is  $\sim 323$  K; desorption clearly occurs at lower  $T$  but this could not be recorded. Such observations are in agreement with the X-ray photoelectron spectroscopy (XPS) studies presented previously by our group;<sup>28</sup> in these experiments, the pressure in the XPS chamber increased significantly when  $C_4C_1(C_3N_2H_2)BF_3$  was introduced, indicating that significant  $C_4C_1(C_3N_2H_2)BF_3$  vaporization was occurring at  $\sim 300$  K.<sup>28</sup> Therefore,  $C_4C_1(C_3N_2H_2)BF_3$  has significantly higher vapor pressure than  $[C_4C_1Im][BF_4]$ .

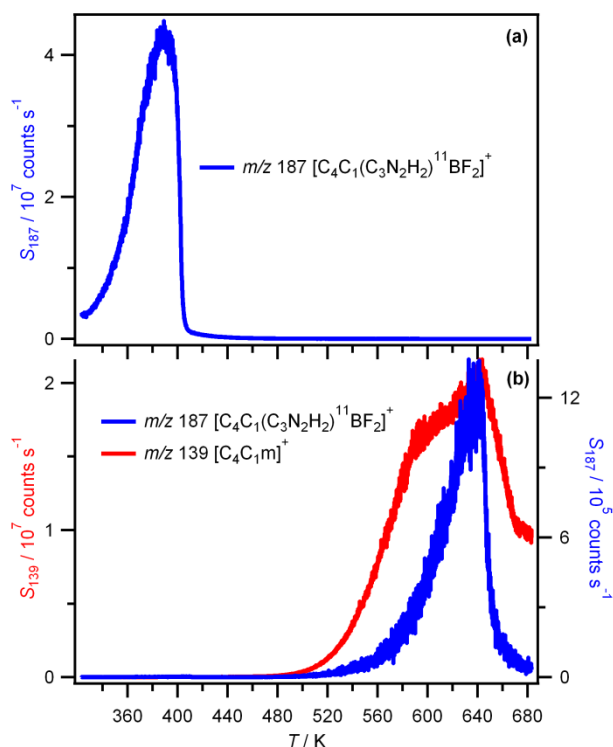


**Figure 5** Positive mode mass spectrum intensity versus  $T$  for the vapor in the DIMS experimental set-up of: (a)  $C_4C_1(C_3N_2H_2)BF_3$  monitoring  $m/z$  187,  $[C_4C_1(C_3N_2H_2)^{11}BF_2]^+$ , (b)  $[C_4C_1Im][BF_4]$  monitoring  $m/z$  139,  $[C_4C_1Im]^+$ , and  $m/z$  187,  $[C_4C_1(C_3N_2H_2)^{11}BF_2]^+$ .

### 3.3 Heating thin films of $[C_4C_1Im][BF_4]$ : *in situ* mass spectrometry of the vapor phase

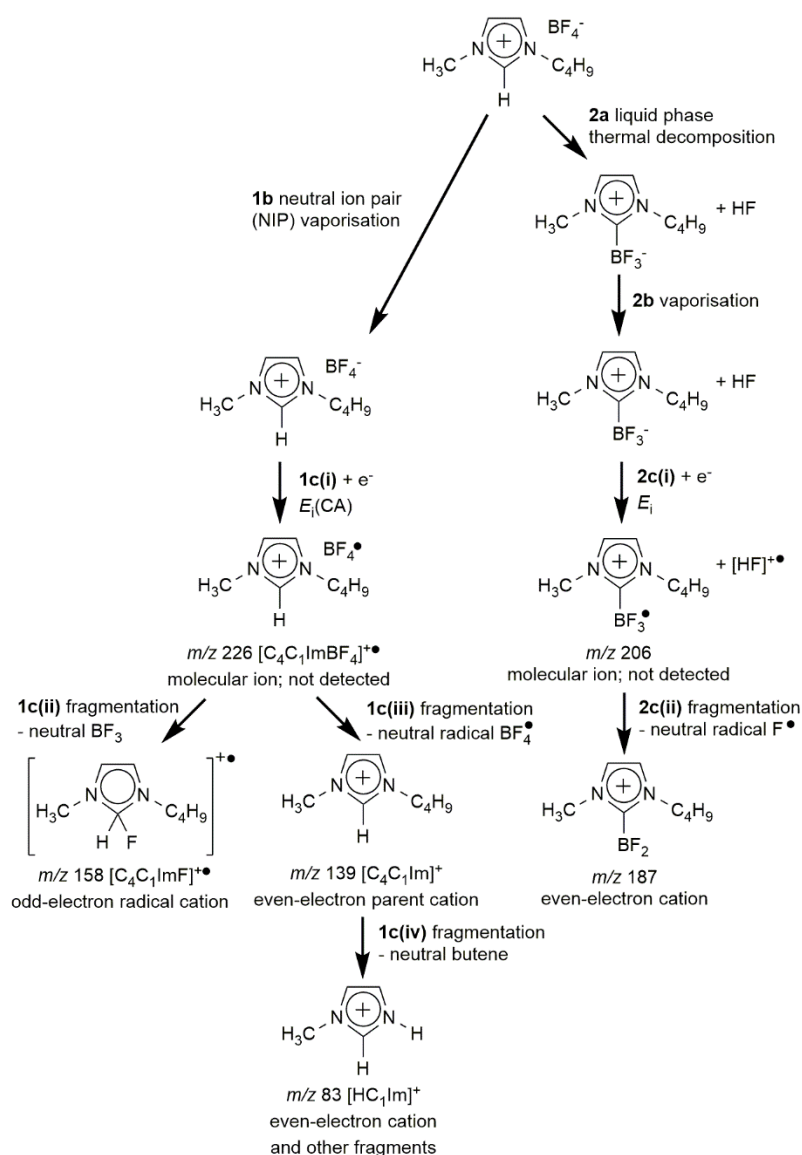
Using DIMS, mass spectra were obtained for  $[C_4C_1Im][BF_4]$  (**Figure 4c-f**). Summaries of the key fragment cations and anions are also given in **Table 2** and **Table 3**. At 500 K (**Figure 4c**), no molecular cation at  $m/z$  226,  $[C_4C_1ImBF_4]^+$ , is observed, as expected based upon previous MS studies of ILs<sup>39</sup> (step 1c(i) in **Scheme 2**). Peaks at  $m/z$  139,  $[C_4C_1Im]^+$ , and  $m/z$  83,  $[HC_1Im]^+$ , confirm vaporization of  $[C_4C_1Im][BF_4]$  NIPs (steps 1c(iii) and 1c(iv) in **Scheme 2** respectively). Clearly, no peaks due to formation of  $C_4C_1(C_3N_2H_2)BF_3$ , *e.g.*,  $m/z$  187, were observed at 500 K. The peak at  $m/z$  158 has been identified previously as the radical cation  $[C_4C_1ImF]^+$ , and is a fragmentation product of ionization of  $[C_4C_1Im][BF_4]$  NIPs (step 1c(ii) in **Scheme 2**).<sup>39</sup> In negative mode at 500 K  $m/z$  86 and  $m/z$  87 are observed, corresponding to  $[^{10}BF_4]^-$  and  $[^{11}BF_4]^-$  respectively (**Figure 4d**). As far as we are aware, this is the first reported observation of the  $[BF_4]^-$  anion in negative mode MS after vaporization of an IL.<sup>33</sup> Overall, these observations confirm that at 500 K under these experimental conditions the vaporization of  $[C_4C_1Im][BF_4]$  NIPs is the dominant process.

At 640 K (**Figure 4e**), in positive mode  $m/z$  139,  $[C_4C_1Im]^+$ , is still present, confirming vaporization of  $[C_4C_1Im][BF_4]$  NIPs. However, an additional peak at  $m/z$  187 is present, corresponding to  $[C_4C_1(C_3N_2H_2)^{11}BF_2]^+$  (step 2c(ii) in **Scheme 2**). Therefore, liquid phase TD is occurring at this temperature, forming  $C_4C_1(C_3N_2H_2)BF_3$ , which is then vaporized. A molecular cation peak at  $m/z$  206,  $[C_4C_1(C_3N_2H_2)BF_3]^+$ , was not observed (step 2c(i) in **Scheme 2**), as expected from the positive mode MS of  $C_4C_1(C_3N_2H_2)BF_3$ . In addition,  $[HF]^+$  at  $m/z$  20 is below the lower  $m/z$  limit for the mass spectrometer. The peaks at  $m/z$  139 and 187 indicate that both vaporization and liquid phase TD were

occurring for  $[\text{C}_4\text{C}_1\text{Im}][\text{BF}_4]$  at 640 K. Negative mode peaks originating from  $\text{C}_4\text{C}_1(\text{C}_3\text{N}_2\text{H}_2)\text{BF}_3$  were not observed in  $[\text{C}_4\text{C}_1\text{Im}][\text{BF}_4]$  MS at 500 K (**Figure 4d**) or 640 K (**Figure 4f**), only peaks associated with the anion are observed at  $m/z$  86 and  $m/z$  87 (*i.e.*  $^{10}\text{BF}_4^-$  and  $^{11}\text{BF}_4^-$ ). This finding is as expected, given that the intensities of the peaks recorded in negative mode MS were significantly lower than those recorded in positive mode MS for the vapor of  $\text{C}_4\text{C}_1(\text{C}_3\text{N}_2\text{H}_2)\text{BF}_3$ , as described previously here.

There is no clear evidence of  $\text{BF}_3$ , a postulated volatile TD product, for which the  $m/z$  49 peak from  $^{11}\text{BF}_2^+$  would be the most intense peak. Furthermore, there is no evidence of proton transfer from the cation to the anion, in particular for the  $\text{C}^2\text{-H}$  proton; no peaks were observed at  $m/z$  138 for a carbene,  $[\text{C}_4\text{C}_1(\text{C}_3\text{N}_2\text{H}_2)]^{+\bullet}$ , or at  $m/z$  88 for  $[\text{HBF}_4]^{+\bullet}$ . It must be noted however that there are no literature EI mass spectra to compare to for these compounds. Therefore, there is no evidence of volatile TD products other than  $\text{C}_4\text{C}_1(\text{C}_3\text{N}_2\text{H}_2)\text{BF}_3$ ; all peaks in the mass spectrum of the vaporized products of  $[\text{C}_4\text{C}_1\text{Im}][\text{BF}_4]$  can be identified as arising from  $[\text{C}_4\text{C}_1\text{Im}][\text{BF}_4]$  NIPs or  $\text{C}_4\text{C}_1(\text{C}_3\text{N}_2\text{H}_2)\text{BF}_3$ . The desorption traces for  $m/z$  139 ( $[\text{C}_4\text{C}_1\text{Im}]^+$  from  $[\text{C}_4\text{C}_1\text{Im}][\text{BF}_4]$  NIPs) and  $m/z$  187 ( $[\text{C}_4\text{C}_1(\text{C}_3\text{N}_2\text{H}_2)^{11}\text{BF}_2]^+$  from  $\text{C}_4\text{C}_1(\text{C}_3\text{N}_2\text{H}_2)\text{BF}_3$ ) with respect to  $T$  are given in **Figure 5b**. Vaporization of  $[\text{C}_4\text{C}_1\text{Im}][\text{BF}_4]$  NIPs occurred at lower  $T$ , before the  $\text{C}_4\text{C}_1(\text{C}_3\text{N}_2\text{H}_2)\text{BF}_3$  signal was observed.

A relatively intense  $m/z$  96 peak was observed for positive mode DIMS of  $[\text{C}_4\text{C}_1\text{Im}][\text{BF}_4]$  at  $T = 500$  K (**Figure 4c**). As no significant amount of  $m/z$  187 (*i.e.* the parent peak for positive mode DIMS of  $\text{C}_4\text{C}_1(\text{C}_3\text{N}_2\text{H}_2)\text{BF}_3$ ) was recorded at this temperature, it can be concluded that the  $m/z$  96 peak was formed by fragmentation after electron ionization for positive mode DIMS of  $[\text{C}_4\text{C}_1\text{Im}][\text{BF}_4]$ . This observation is in agreement with LOSMS experiments for  $[\text{C}_n\text{C}_1\text{Im}][\text{BF}_4]$  ( $n = 4, 8$ ), where an  $m/z$  96 peak was observed and no  $m/z$  187 peak was observed.<sup>39</sup>



**Scheme 2** (a) Liquid phase thermal decomposition (TD), (b) vaporization, (c) electron ionization (EI) and fragmentation taking place in the vapor phase inside the mass spectrometer for [C<sub>4</sub>C<sub>1</sub>Im][BF<sub>4</sub>]. Route 1 is for neutral ion pair (NIP) vaporization, and route 2 is for liquid phase TD to form C<sub>4</sub>C<sub>1</sub>(C<sub>3</sub>N<sub>2</sub>H<sub>2</sub>)BF<sub>3</sub> followed by vaporization of C<sub>4</sub>C<sub>1</sub>(C<sub>3</sub>N<sub>2</sub>H<sub>2</sub>)BF<sub>3</sub>.

### 3.4 Heating bulk [C<sub>n</sub>C<sub>1</sub>Im][PF<sub>6</sub>] followed by *ex situ* characterization of the condensate

Vaporization + condensation experiments were repeated with 1-alkyl-3-methylimidazolium hexafluorophosphate ILs, [C<sub>n</sub>C<sub>1</sub>Im][PF<sub>6</sub>] (where *n* = 4 or 8), to investigate the formation of TD products. [C<sub>4</sub>C<sub>1</sub>Im][PF<sub>6</sub>] was heated at 641 K in the vaporization + condensation apparatus and the condensates and residue were analyzed by <sup>1</sup>H NMR spectroscopy. The condensate contained 89% C<sub>4</sub>C<sub>1</sub>(C<sub>3</sub>N<sub>2</sub>H<sub>2</sub>)PF<sub>5</sub>, 8% [C<sub>4</sub>C<sub>1</sub>Im][PF<sub>6</sub>], and 3% unknown products. The residue was found to contain 96% [C<sub>4</sub>C<sub>1</sub>Im][PF<sub>6</sub>], 2% C<sub>4</sub>C<sub>1</sub>(C<sub>3</sub>N<sub>2</sub>H<sub>2</sub>)PF<sub>5</sub>, and 2% unknown products. As with [C<sub>4</sub>C<sub>1</sub>Im][BF<sub>4</sub>], the TD product, C<sub>4</sub>C<sub>1</sub>(C<sub>3</sub>N<sub>2</sub>H<sub>2</sub>)PF<sub>5</sub>, was obtained as the major product at relatively high temperature. The presence of C<sub>4</sub>C<sub>1</sub>(C<sub>3</sub>N<sub>2</sub>H<sub>2</sub>)PF<sub>5</sub> in the residue indicates TD of the IL occurs in the liquid phase, before vaporization. In the event of a vapor phase TD, condensation of the TD product into the residue is unlikely at these

temperatures given the significantly higher  $\Delta_{\text{vap}}H$  of the TD product relative to the IL, as demonstrated in **Figure 5**. The small amount of  $[\text{C}_4\text{C}_1\text{Im}][\text{PF}_6]$  in the condensate also indicates that IL vaporization occurs as a competing process during the vaporization + condensation experiments.

$[\text{C}_8\text{C}_1\text{Im}][\text{PF}_6]$  was also heated in the vaporization + condensation apparatus at 625 K and the condensate was found to contain 65%  $\text{C}_8\text{C}_1(\text{C}_3\text{N}_2\text{H}_2)\text{PF}_5$ , 31%  $[\text{C}_8\text{C}_1\text{Im}][\text{PF}_6]$  and 3% unknown product. The residue was also found to contain 93%  $[\text{C}_8\text{C}_1\text{Im}][\text{PF}_6]$ , 2%  $\text{C}_8\text{C}_1(\text{C}_3\text{N}_2\text{H}_2)\text{PF}_5$ , and 5% unknown products. Although  $\text{C}_8\text{C}_1(\text{C}_3\text{N}_2\text{H}_2)\text{PF}_5$  was the major product, the  $[\text{C}_8\text{C}_1\text{Im}][\text{PF}_6]$  condensate contained less TD product and more IL than the  $[\text{C}_4\text{C}_1\text{Im}][\text{PF}_6]$  condensate. As the condensation temperature was slightly lower for  $[\text{C}_8\text{C}_1\text{Im}][\text{PF}_6]$  (albeit by 16 K), IL vaporization should be favored over TD; however, longer alkyl chain ILs have higher  $\Delta_{\text{vap}}H$  values,<sup>33</sup> suggesting less IL should be collected in the condensate. Interestingly, the  $[\text{C}_8\text{C}_1\text{Im}][\text{PF}_6]$  residue contained only 2%  $\text{C}_8\text{C}_1(\text{C}_3\text{N}_2\text{H}_2)\text{PF}_5$ , the same proportion as the higher temperature  $[\text{C}_4\text{C}_1\text{Im}][\text{PF}_6]$  condensate. This composition suggests that the vaporization of the TD product is a fast process under these experimental conditions. However, the large volume of IL has a low surface area to bulk ratio which hinders vaporization of the TD products, resulting in a small portion remaining in the liquid phase. As both  $\text{C}_8\text{C}_1(\text{C}_3\text{N}_2\text{H}_2)\text{PF}_5$  and  $[\text{C}_8\text{C}_1\text{Im}][\text{PF}_6]$  are condensed, there is competition between IL vaporization and liquid phase TD (followed by vaporization of the TD product). Tian *et al.* observed the formation of  $\text{C}_1\text{C}_1(\text{C}_3\text{N}_2\text{H}_2)\text{PF}_5$  for  $[\text{C}_1\text{C}_1\text{Im}][\text{PF}_6]$ , but no IL vaporization was reported.<sup>29</sup> Therefore, these results appear contradictory.

### 3.5 Heating thin films of $\text{C}_n\text{C}_1(\text{C}_3\text{N}_2\text{H}_2)\text{PF}_5$ : *in situ* mass spectrometry of the vapor phase

To understand the MS of  $\text{C}_n\text{C}_1(\text{C}_3\text{N}_2\text{H}_2)\text{PF}_5$  a small portion of  $\text{C}_4\text{C}_1(\text{C}_3\text{N}_2\text{H}_2)\text{PF}_5$  was purified and introduced to the mass spectrometer (**Figure 6**). A list of key cation and anion fragments are also given in **Table 2** and **Table 3**. The peaks at  $m/z$  137,  $m/z$  95 and  $m/z$  82 (**Figure 6a**) are fragments of  $\text{C}_4\text{C}_1(\text{C}_3\text{N}_2\text{H}_2)\text{PF}_5$  which were also observed for  $\text{C}_4\text{C}_1(\text{C}_3\text{N}_2\text{H}_2)\text{BF}_3$  (**Figure 4a**). The peak at  $m/z$  245 is  $[\text{C}_4\text{C}_1(\text{C}_3\text{N}_2\text{H}_2)\text{PF}_4]^+$ , a fragmentation product of  $\text{C}_4\text{C}_1(\text{C}_3\text{N}_2\text{H}_2)\text{PF}_5$  minus one fluorine (**Scheme S1**, step 2c(ii); analogous to **Scheme 2**, step 2c(ii)). Again, no peak for the  $\text{C}_4\text{C}_1(\text{C}_3\text{N}_2\text{H}_2)\text{PF}_5$  molecular ion,  $[\text{C}_4\text{C}_1(\text{C}_3\text{N}_2\text{H}_2)\text{PF}_5]^+$ , was observed at  $m/z$  264. The peak at  $m/z$  245 was chosen to monitor  $\text{C}_4\text{C}_1(\text{C}_3\text{N}_2\text{H}_2)\text{PF}_5$  vaporization with respect to temperature (**Figure 6b**). Significant vaporization of  $\text{C}_4\text{C}_1(\text{C}_3\text{N}_2\text{H}_2)\text{PF}_5$  also occurs at low temperature (e.g.  $\sim 323$  K); however, at  $T > 360$  K the  $[\text{C}_4\text{C}_1(\text{C}_3\text{N}_2\text{H}_2)\text{PF}_4]^+$  signal rapidly increases and desorption is completed by 423 K. Therefore, the vapor pressure of  $\text{C}_4\text{C}_1(\text{C}_3\text{N}_2\text{H}_2)\text{PF}_5$  is higher than the vapor pressure of the IL as desorption occurs at the lowest temperature in this setup ( $\approx 2.5 \times 10^{-6}$  mbar base pressure). Unlike for  $\text{C}_4\text{C}_1(\text{C}_3\text{N}_2\text{H}_2)\text{BF}_3$ , a dimer signal at  $m/z$  509 was not observed for  $\text{C}_4\text{C}_1(\text{C}_3\text{N}_2\text{H}_2)\text{PF}_5$ , even at elevated temperatures (**Figure S9**).

A relatively intense  $m/z$  96 peak was observed for positive mode DIMS of  $\text{C}_4\text{C}_1(\text{C}_3\text{N}_2\text{H}_2)\text{PF}_5$  (**Figure 6a**). Therefore, this  $m/z$  96 peak was a fragmentation product of  $\text{C}_4\text{C}_1(\text{C}_3\text{N}_2\text{H}_2)\text{PF}_5$ .

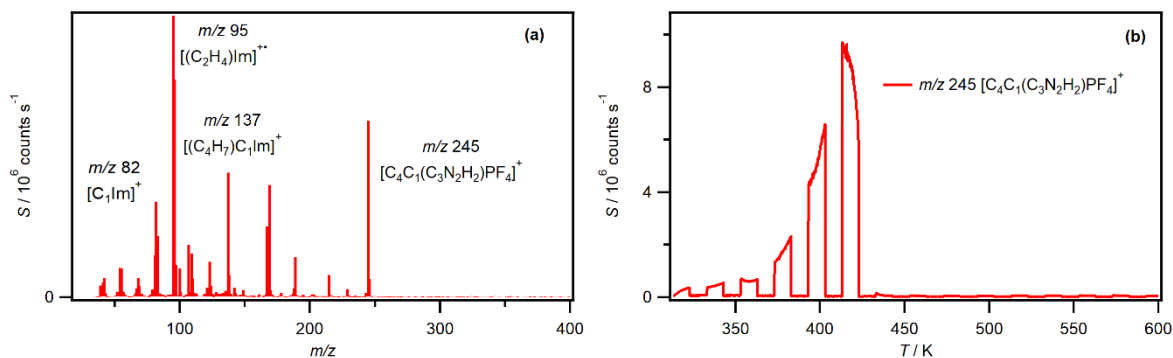


**Figure 6** (a) Positive mode mass spectrum intensity versus  $m/z$  for  $C_4C_1(C_3N_2H_2)PF_5$  at 313 K. (b) Positive mode mass spectrum intensity versus  $T$  for  $[C_4C_1(C_3N_2H_2)PF_4]^+$   $m/z$  245. The block profile is due to positive-negative mode switching during measurements.

### 3.6 Heating thin films of $[C_nC_1Im][PF_6]$ : *in situ* mass spectrometry of the vapor phase

Mass spectra of  $[C_4C_1Im][PF_6]$  (**Figure 7a-d**) were also measured to investigate the *in situ* formation of  $C_4C_1(C_3N_2H_2)PF_5$ . As expected, no molecular cation at  $m/z$  284,  $[C_4C_1ImPF_6]^+$ , is observed at high or low temperatures. The peaks at  $m/z$  139,  $[C_4C_1Im]^+$ , and  $m/z$  83,  $[HC_1Im]^+$ , again confirm vaporization of  $[C_4C_1Im][PF_6]$  NIPs and at 493 K  $C_4C_1(C_3N_2H_2)PF_5$ , *e.g.*,  $m/z$  245, is not observed. The negative mode MS at both 493 K and 623 K (**Figure 7b, d**) only show a signal corresponding to the  $[PF_6]^-$  anion at  $m/z$  145; this fragmentation pattern matches a literature report<sup>42</sup>. Again, these observations confirm that at  $T = 493$  K under these spectrometer conditions the vaporization of  $[C_4C_1Im][PF_6]$  NIPs is the dominant process. At higher  $T$ , *e.g.* 623 K, in positive mode (**Figure 7c**) signals corresponding to the NIPs are still present. A small peak at  $m/z$  245,  $[C_4C_1(C_3N_2H_2)PF_4]^+$ , appears, however the signal is extremely low; an expansion of the baseline has been presented. This signal indicates liquid phase TD is occurring to form  $C_4C_1(C_3N_2H_2)PF_5$ . However, under the spectrometer conditions used here, vaporization of  $[C_4C_1Im][PF_6]$  is the dominant process; the large surface area to bulk ratio allows  $[C_4C_1Im][PF_6]$  to evaporate before significant TD can occur in the liquid phase.



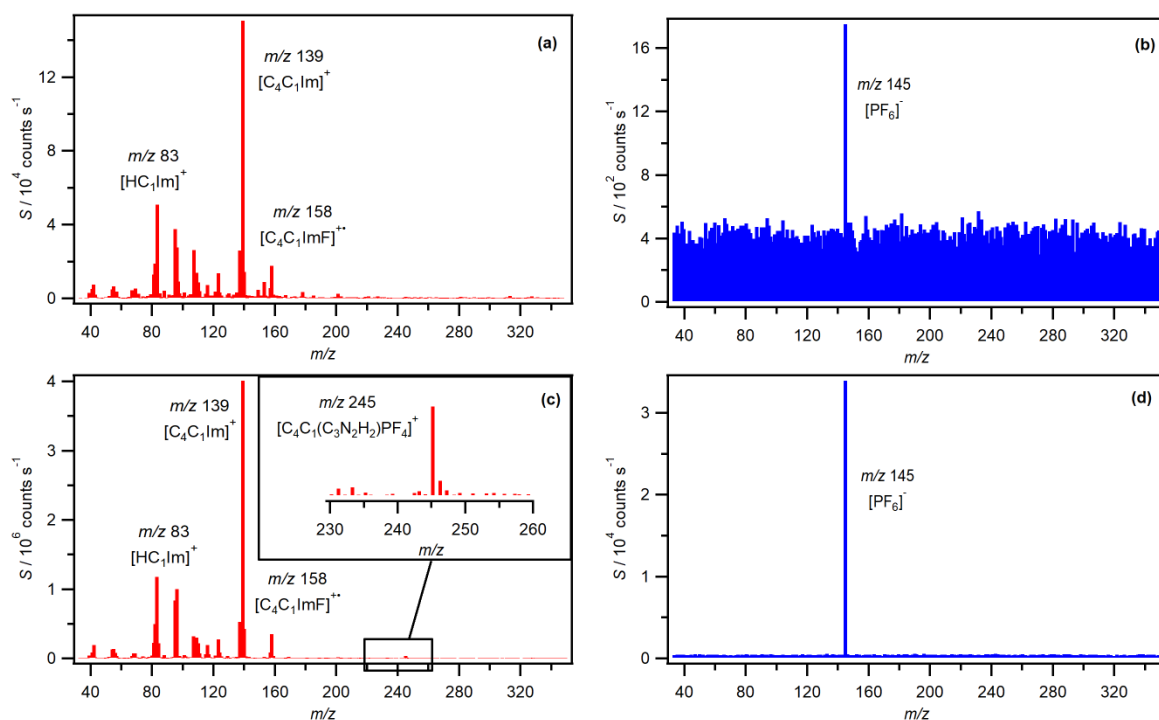


**Figure 7** Mass spectrum intensity versus  $m/z$  for  $[C_4C_1Im][PF_6]$ : (a) positive mode at 493 K, (b) negative mode at 503 K, (c) positive mode at 623 K, (d) negative mode at 623 K.

$[C_8C_1Im][PF_6]$  was also investigated by DIMS (**Figure 8a-d**) to investigate alkyl chain length effects within this setup. At 533 K (**Figure 8a**), no molecular cation at  $m/z$  340,  $[C_8C_1ImPF_6]^{+*}$ , is observed, as expected. Peaks at  $m/z$  195,  $[C_8C_1Im]^+$ , and  $m/z$  83,  $[HC_1Im]^+$ , again confirm vaporization of  $[C_8C_1Im][PF_6]$  NIPs. The small  $m/z$  257 peak in the positive mode at 533 K could not be identified; it is not present in the positive mode spectrum at 543 K. In negative mode the  $[PF_6]^-$  anion,  $m/z$  145, was the only signal observed at both 543 K and 623 K (**Figure 8b and d**). At 543 K (**Figure 8c**), the positive mode MS of  $[C_4C_1Im][PF_6]$  is similar to the positive mode spectrum at 533 K. However, a peak at  $m/z$  301 is present which corresponds to  $[C_8C_1(C_3N_2H_2)PF_4]^+$ , a fragmentation product of  $C_8C_1(C_3N_2H_2)PF_5$ . Therefore, liquid phase TD is occurring to form  $C_8C_1(C_3N_2H_2)PF_5$ , followed by  $C_8C_1(C_3N_2H_2)PF_5$  vaporization at 633 K inside the spectrometer. No molecular cation at  $m/z$  320,  $[C_8C_1(C_3N_2H_2)PF_5]^{+*}$ , is observed, as with  $C_4C_1(C_3N_2H_2)BF_3$  and  $C_4C_1(C_3N_2H_2)PF_5$ . Relative to  $[C_4C_1(C_3N_2H_2)PF_4]^+$  at  $m/z$  245, the peak at  $m/z$  301 appears to have a higher intensity relative to the parent cation of the ILs. There are a number of possible explanations for this observation.

A relatively intense  $m/z$  96 peak was observed for positive mode DIMS of  $[C_8C_1Im][PF_6]$  at  $T = 533$  K (**Figure 7a**). As no significant amount of  $m/z$  301 (*i.e.* the parent peak for positive mode DIMS of  $C_8C_1(C_3N_2H_2)PF_5$ ) was recorded at this temperature, it can be concluded that the  $m/z$  96 peak was formed by fragmentation after electron ionization for positive mode DIMS of  $[C_8C_1Im][PF_6]$ .

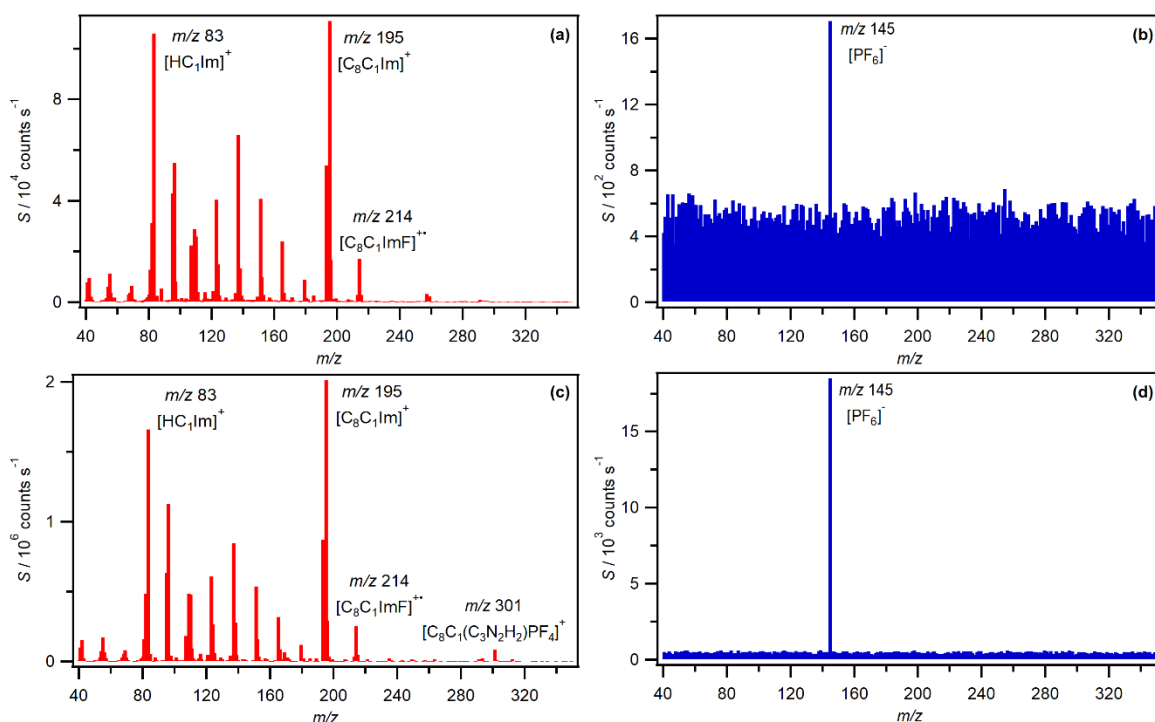


**Figure 8** Mass spectrum intensity versus  $m/z$  for  $[C_8C_1Im][PF_6]$ : (a) positive mode at 533 K, (b) negative mode at 543 K, (c) positive mode at 623 K, (d) negative mode at 623 K.

**Table 2** Cations observed in positive mode MS of  $[C_4C_1Im][BF_4]$ ,  $[C_nC_1Im][PF_6]$ ,  $C_4C_1(C_3N_2H_2)BF_3$ , and  $C_4C_1(C_3N_2H_2)PF_5$ .

$m/z$	Formula	Notation	Source
82	$[(C_3H_3N_2)CH_3]^{++}$	$[C_1Im]^{++}$	All samples
83	$[H(C_3H_3N_2)CH_3]^+$	$[HC_1Im]^+$	All samples
95	$[C_2H_4(C_3H_3N_2)]^+$	$[(C_2H_4)Im]^+$	All samples
96	$[C_2H_5(C_3H_3N_2)]^{++}$	$[C_2Im]^{++}$	All samples
137	$[C_4H_7(C_3H_3N_2)CH_3]^+$	$[(C_4H_7)C_1Im]^+$	All samples
139	$[C_4H_9(C_3H_3N_2)CH_3]^+$	$[C_4C_1Im]^+$	$[C_4C_1Im][BF_4]$ $[C_4C_1Im][PF_6]$
158	$[C_4H_9(C_3H_3N_2)CH_3F]^{++}$	$[C_4C_1ImF]^{++}$	$[C_4C_1Im][BF_4]$ $[C_4C_1Im][PF_6]$
187	$[C_4H_9CH_3(C_3N_2H_2)BF_2]^+$	$[C_4C_1(C_3N_2H_2)BF_2]^+$	$C_4C_1(C_3N_2H_2)BF_3$ $[C_4C_1Im][BF_4]$
195	$[C_8H_{17}(C_3H_3N_2)CH_3]^+$	$[C_8C_1Im]^+$	$[C_8C_1Im][PF_6]$
214	$[C_8H_{17}(C_3H_3N_2)CH_3F]^{++}$	$[C_8C_1ImF]^{++}$	$[C_8C_1Im][PF_6]$
245	$[C_4H_9CH_3(C_3N_2H_2)PF_4]^+$	$[C_4C_1(C_3N_2H_2)PF_4]^+$	$C_4C_1(C_3N_2H_2)PF_5$ $[C_4C_1Im][PF_6]$
301	$[C_8H_{17}CH_3(C_3N_2H_2)PF_4]^+$	$[C_8C_1(C_3N_2H_2)PF_4]^+$	$[C_8C_1Im][PF_6]$
393	$[C_4H_9CH_3(C_3N_2H_2)BF_2(C_4C_1(C_3N_2H_2)BF_3)]^+$	$[C_4C_1(C_3N_2H_2)BF_2(C_4C_1(C_3N_2H_2)BF_3)]^+$	$C_4C_1(C_3N_2H_2)BF_3$

**Table 3** Anions observed in negative mode MS of  $[C_4C_1Im][BF_4]$ ,  $[C_nC_1Im][PF_6]$ ,  $C_4C_1(C_3N_2H_2)BF_3$ , and  $C_4C_1(C_3N_2H_2)PF_5$ .

$m/z$	Formula	Notation	Source
81	$[CH_3(C_3N_2H_2)]^-$	$[C_1(C_3N_2H_2)]^-$	$C_4C_1(C_3N_2H_2)BF_3$

86	$[^{10}\text{BF}_4]^-$	$[\text{BF}_4]^-$	$[\text{C}_4\text{C}_1\text{Im}][\text{BF}_4]$
87	$[^{11}\text{BF}_4]^-$	$[\text{BF}_4]^-$	$[\text{C}_4\text{C}_1\text{Im}][\text{BF}_4]$
145	$[\text{PF}_6]^-$	$[\text{PF}_6]^-$	$[\text{C}_4\text{C}_1\text{Im}][\text{PF}_6]$
			$[\text{C}_8\text{C}_1\text{Im}][\text{PF}_6]$
149	$[\text{CH}_3(\text{C}_3\text{N}_2\text{H}_2)^{11}\text{BF}_3]^-$	$[\text{C}_1(\text{C}_3\text{N}_2\text{H}_2)^{11}\text{BF}_3]^-$	$\text{C}_4\text{C}_1(\text{C}_3\text{N}_2\text{H}_2)\text{BF}_3$
205	$[\text{C}_4\text{H}_9\text{CH}_3(\text{C}_3\text{N}_2\text{H})^{11}\text{BF}_3]^-$	$[\text{C}_4\text{C}_1(\text{C}_3\text{N}_2\text{H})^{11}\text{BF}_3]^-$	$\text{C}_4\text{C}_1(\text{C}_3\text{N}_2\text{H}_2)\text{BF}_3$

## 4. Discussion

Measuring DIM spectra of  $\text{C}_4\text{C}_1(\text{C}_3\text{N}_2\text{H}_2)\text{BF}_3$  and  $\text{C}_n\text{C}_1(\text{C}_3\text{N}_2\text{H}_2)\text{PF}_5$  allowed identification of MS peaks which originate solely from these TD products. Peaks were clearly identified as being from these TD products in the positive mode DIM spectra of  $\text{C}_4\text{C}_1(\text{C}_3\text{N}_2\text{H}_2)\text{BF}_3$  ( $m/z$  187) and  $\text{C}_4\text{C}_1(\text{C}_3\text{N}_2\text{H}_2)\text{PF}_5$  ( $m/z$  245). No peaks at lower  $m/z$  than that of the  $[\text{C}_4\text{C}_1\text{Im}]^+$  cation,  $m/z$  139, were positively identified as only coming from ionization of either  $\text{C}_4\text{C}_1(\text{C}_3\text{N}_2\text{H}_2)\text{BF}_3$  or  $\text{C}_n\text{C}_1(\text{C}_3\text{N}_2\text{H}_2)\text{PF}_5$ . Therefore, only the peaks at  $m/z$  187 and  $m/z$  245 were used to identify vaporization of TD products for MS of the ILs studied here. HF was not detected in either experimental set-up used here. When heating  $[\text{C}_4\text{C}_1\text{Im}][\text{BF}_4]$  and  $[\text{C}_n\text{C}_1\text{Im}][\text{PF}_6]$  in the bulk vaporization + condensation apparatus the HF will have either: been trapped by the diffusion pump (as HF is very volatile it will not have readily condensed) or reacted with the glass walls/steel tubing. The DIMS system was not capable of detecting HF (due to the low  $m/z$  value of  $[\text{HF}]^{+*}$ ).

There are two possible reasons why  $\text{C}_n\text{C}_1(\text{C}_3\text{N}_2\text{H}_2)\text{BF}_3$  or  $\text{C}_n\text{C}_1(\text{C}_3\text{N}_2\text{H}_2)\text{PF}_5$  were not observed in previous experiments on the vapor of  $[\text{C}_n\text{C}_1\text{Im}][\text{BF}_4]$  and  $[\text{C}_n\text{C}_1\text{Im}][\text{PF}_6]$ . Firstly, the particular TD product was not present in significant quantities in the vapor phase. This was the case for  $[\text{C}_n\text{C}_1\text{Im}][\text{BF}_4]$ ; no peaks due to  $\text{C}_n\text{C}_1(\text{C}_3\text{N}_2\text{H}_2)\text{BF}_3$  were observed when LOSMS was used.<sup>39</sup> Secondly, identification of the peaks due to ionization of the TD products is difficult. For both  $\text{C}_4\text{C}_1(\text{C}_3\text{N}_2\text{H}_2)\text{BF}_3$  and  $\text{C}_4\text{C}_1(\text{C}_3\text{N}_2\text{H}_2)\text{PF}_5$ , the parent ions observed after electron ionization are not easy to interpret without prior knowledge of the expected TD products. The loss by fragmentation of a fluorine radical,  $\text{F}^*$ , after electron ionization to give an unexpected parent ion is not an obvious ion to form from IL vapor. It is possible that a peak of relatively low intensity may have been ignored during data analysis. Hence, *ex situ* TD product preparation is perfectly complimentary to *in situ* MS detection. For two previously published studies on the identification of the species vaporized after heating  $[\text{C}_4\text{C}_1\text{Im}][\text{PF}_6]$  using electron ionization MS, neither study presented the appropriate regions of their mass spectra to determine if the TD products were present or not.<sup>27, 42</sup>

No significant quantities of TD products were found in the residue in the bulk apparatus, other than remaining  $\text{C}_n\text{C}_1(\text{C}_3\text{N}_2\text{H}_2)\text{BF}_3$  or  $\text{C}_n\text{C}_1(\text{C}_3\text{N}_2\text{H}_2)\text{PF}_5$ . Furthermore, no visible quantity of sample was left in the glass vial after each DIMS experiment. These observations confirm that no significant quantity of non-volatile TD product was formed during either the bulk heating experiments or the DIMS experiments. All experiments were performed in systems with base pressures of  $\approx 10^{-6}$  mbar. Therefore, the amount of water present during the experiments was minimal,<sup>68</sup> meaning that TD via hydrolysis can be ruled out as the major TD mechanism.

Volpe *et al.* used their MS evidence to conclude that 1-ethylimidazole was a TD product of  $[C_4C_1Im][PF_6]$ .<sup>27</sup> No 1-ethylimidazole (or similar TD products) were detected either in the condensates or the residues; previous experiments suggest that both  $[C_nC_1Im][BF_4]$  and  $[C_nC_1Im][PF_6]$  thermally decompose to give neutral 1-alkylimidazoles<sup>19, 20, 27</sup>. There are two possible reasons for this observation, neither of which can be ruled out: firstly, that 1-ethylimidazole and other TD products were not formed under the reaction conditions used here; secondly, such TD products were formed, but were sufficiently volatile that they did not condense in the bulk apparatus used here. For all DIMS experiments presented here, a peak at  $m/z$  96 was observed (**Table 2**, line 5). Therefore, the match of the peak at  $m/z$  96 to that of the parent ion of 1-ethylimidazole is insufficient evidence for assignment. The appearance energy evidence from Volpe *et al.* strongly suggests that their peak at  $m/z$  96 was formed from a TD product, not from IL NIPs.<sup>27</sup> However, their peak at  $m/z$  96 could be formed by fragmentation after electron ionization of the zwitterion TD product. The mass spectra presented by Volpe *et al.* do not show the region where the zwitterion peak at  $m/z$  245 would have occurred, if present.<sup>27</sup> Overall, an answer cannot be provided at this stage; it is possible that  $[C_nC_1Im][PF_6]$  ILs thermally decompose via two different mechanisms, one that gives 1-ethylimidazole and one that gives a zwitterion. However, it is also possible that the  $m/z$  96 peak observed by Volpe *et al.* was produced by fragmentation of  $[C_nC_1Im][PF_6]$  NIPs after electron ionization.

For TD product formation followed by vaporization, the overall process can be separated into two steps: liquid phase TD (controlled by  $E_{a,TD}$ ), and vaporization of the liquid phase TD products, controlled by  $\Delta_{vap}H_{298}$  (TD products). Both  $C_4C_1(C_3N_2H_2)BF_3$  and  $C_4C_1(C_3N_2H_2)PF_5$  TD products showed significant vaporization at 323 K in the DIMS setup. However, in both the bulk heating experiments and the DIMS experiments on the ILs, significant TD product formation is not detected at low temperatures. This is highlighted by **Figure 5**, which shows the temperature profiles of pure  $C_4C_1(C_3N_2H_2)BF_3$  (isolated and characterized by *ex situ* vaporization + condensation experiments) and TD of  $[C_4C_1Im][BF_4]$  (*i.e.* in situ formation). As liquid phase TD occurred at more than 200 K above  $C_4C_1(C_3N_2H_2)BF_3$  vaporization, it can be concluded that  $\Delta_{vap}H_{298}(\text{TD product}) \ll E_{a,TD}$ . Therefore, the rate-determining step for TD product formation followed by vaporization was  $E_{a,TD}$ . Consequently, TD product vaporization is almost instantaneous after TD product formation; hence, the zwitterionic TD products have significantly weaker intermolecular interactions than the ILs. Vaporization of the NIPs occurs at much lower temperatures than liquid phase TD. Therefore, it can also be concluded that for  $[C_4C_1Im][BF_4]$  and  $[C_nC_1Im][PF_6]$  (where  $n = 4$  and  $8$ )  $\Delta_{vap}H_{298}(\text{IL NIP}) \ll E_{a,TD}$ .  $\Delta_{vap}H_{298}$  for  $[C_4C_1Im][BF_4]$  and  $[C_4C_1Im][PF_6]$  are both  $\sim 150 \text{ kJ mol}^{-1}$ ,<sup>27, 33, 34, 40, 60</sup> indicating that  $E_{a,TD}$  for these two ILs are likely to be towards  $200 \text{ kJ mol}^{-1}$ .

The thermal stability literature for dialkylimidazolium  $[BF_4]^-$  and  $[PF_6]^-$  ILs appears to be contradictory. It is unclear under what conditions IL vaporization or TD will occur. There are reports of TD,<sup>13-17, 19, 20</sup> IL vaporization,<sup>34, 36, 39, 40, 42, 60, 61, 66</sup> and competition between the two in this work and others.<sup>27, 28</sup> Many of these studies assume either decomposition or vaporization, without considering both processes occurring in competition. Techniques employing MS are advantageous in this regard, especially over other approaches that are unable to definitively identify the composition of the vapor, e.g. most TGA studies assume TD without vaporization. Importantly, a key question to answer is: if IL vaporization is energetically more favorable than liquid phase TD, why is the major product of heating  $[C_nC_1Im][BF_4]$  or  $[C_nC_1Im][PF_6]$  under certain experimental conditions the zwitterionic TD product and not intact IL? Based on literature data and our results, we propose that there are two key factors controlling the

competition between IL vaporization and TD product formation + vaporization: single versus multiple vaporization events and sample geometry. To understand both of these factors, it is vital to consider the vaporization approach used, which depends on experimental conditions.

There are two extremes of approach for IL vaporization studies: Langmuir vaporization (**Figure 9**) and effusive vaporization (**Figure 9**). Firstly, Langmuir vaporization involves free vaporization from a liquid surface to the detector/condensation region; the detector/condensation region is in line-of-sight with the whole IL sample surface. This approach has been successfully used for ILs, *e.g.* LOSMS<sup>22, 34-40, 69</sup> and quartz crystal microbalance, QCM<sup>60, 66, 70-85</sup>. Effusive conditions involve near-equilibrium vaporization, usually achieved in a Knudsen effusion cell with a small orifice hole, which enables gas-phase saturation by slowing the escape of vaporized species.<sup>27, 51-55, 70, 86-94</sup> It is important to note that the liquid phase TD products are sufficiently volatile (*i.e.* relatively small  $\Delta_{\text{vap}}H$ ) that the multiple vaporization events are not a limiting process ( $E_{\text{a,TD}}$  is the rate limiting step), whereas for IL NIPs, condensation followed by re-vaporization must overcome the significantly larger  $\Delta_{\text{vap}}H$  of ILs.

The sample geometry, *i.e.* the sample surface area:volume ratio, matters because vaporization is a surface process and TD is a bulk process. Another way of considering this ratio is the number of IL ion pairs at the surface relative to the number of IL ion pairs in the bulk liquid. A lower surface area:volume ratio favors TD, whereas a higher surface area:volume ratio favors IL NIP vaporization.

Certain apparatus involve a single vaporization event (*i.e.* Langmuir apparatus), whereas other apparatus involve, on average, multiple vaporization events to achieve the same signal level as single vaporization event apparatus (*i.e.* effusion apparatus). Therefore, to achieve the same signal (or sample amount) at the detector (or condensation region), more energy (*i.e.* higher temperature) is required for effusion apparatus compared to Langmuir apparatus. The need for a higher temperature in the effusion apparatus means that the probability of TD occurring increases, relative to the probability of IL NIP vaporization. Another way to think of this reasoning is that effusion apparatus has a smaller effective sample surface area that is in line of sight with the detector/condensation region to Langmuir apparatus.

The DIMS apparatus gave a single/low number of vaporization events (**Figure 9b**). The mass spectrometer ionization region was in line-of-sight with the IL sample, but the IL that vaporized may hit the glass wall before reaching the mass spectrometer ionization region. Such IL NIPs would need to re-vaporize (at least once more) to reach the mass spectrometer ionization region. As the collection vessel in the vaporization + condensation apparatus is not in line-of-sight, multiple vaporization events were required for certain, given the design of the apparatus with a curve between the sample and the sample collection region (**Figure 9c**). Therefore, the vaporization + condensation apparatus was likely to give more TD (relative to IL NIP vaporization), relative to the DIMS apparatus.

To maximize the probability of observing IL NIP vaporization, at least for  $[\text{C}_n\text{C}_1\text{Im}][\text{BF}_4]$  and  $[\text{C}_n\text{C}_1\text{Im}][\text{PF}_6]$ , the sample surface area:volume ratio must be maximized (*i.e.* use very thin films), along with an apparatus geometry which allows only single vaporization events (*i.e.* line-of-sight). Conversely, to maximize the probability of observing IL liquid phase TD the sample surface area:volume ratio must be minimized (*i.e.* use thicker films), along with an apparatus geometry which

favors multiple vaporization events (*i.e.* a Knudsen cell, or at least one bend between sample and detector).

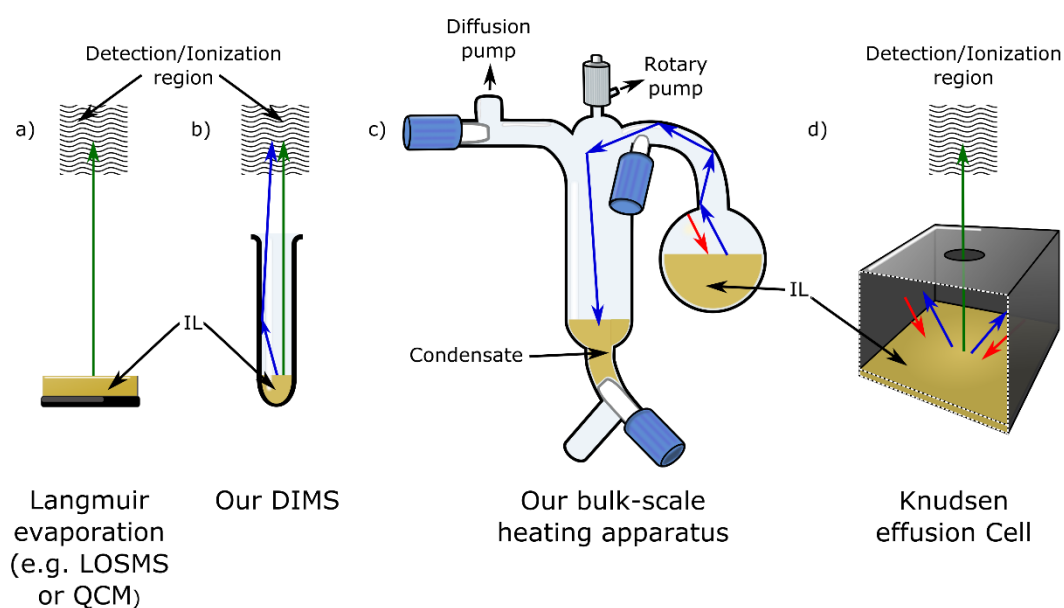


**Figure 9** Schematics showing the vaporization steps for the three different experimental set-ups: (a) LOSMS, (b) DIMS, (c) vaporization + condensation apparatus, (d) Knudsen effusion cell. The green arrows represent one step vaporization from sample to detection region, *i.e.* Langmuir/free vaporization. The blue arrows represent multiple vaporization steps from sample to detection region, *i.e.* more closely representing an effusive experimental set-up. The red arrow represents vaporization of IL from the wall of the vaporization + condensation apparatus back onto the sample surface, hindering further IL vaporization.

## 5. Conclusions

The bulk vaporization + condensation experiments of  $[C_4C_1Im][BF_4]$  and  $[C_nC_1Im][PF_6]$  gave mixtures of IL and the respective TD products  $C_4C_1(C_3N_2H_2)BF_3$  and  $C_nC_1(C_3N_2H_2)PF_5$  (where  $n = 4$  or  $8$ ). DIMS of the purified TD products then enabled the identification of their characteristic MS signals. Importantly, the TD products do not have distinct signals from their respective ILs, except in the positive mode at  $m/z$  higher than the corresponding IL cations,  $[C_nC_1Im]^+$ . These signals were subsequently observed *in situ* when analyzing the respective ILs by DIMS, along with signals originating from NIPS, indicating competing vaporization and decomposition. Previous studies have not reported the signals originating from the TD product reported in this work, possibly due to restricted  $m/z$  values. Furthermore, identifying the TD products without prior knowledge of the vaporized species would be difficult, hence our *ex situ* preparation is perfectly complimentary to *in situ* detection. The results presented here show that sample surface area to volume ratios and heating rates are critical experimental parameters for ILs that show competition between vaporization and thermal decomposition. These experimental factors have been explained in terms of Langmuir evaporation and Knudsen effusion-like conditions, allowing us to draw together observations from previous studies to make sense of the literature on IL thermal stability. Describing the experimental setup, particularly in terms of sample holders and sample volume, is therefore important for future IL TD or vaporization studies.

## 6. Acknowledgments

K.R.J.L acknowledges the Royal Society for the award of a University Research Fellowship. C.J.C, S.P., A.W.T and P.L. thank EPSRC for support EP/D073014/1, EP/I018093/1 and EP/K005138/1. The authors thank Prof Sir Martyn Poliakoff FRS for access to the Thermo Finnigan PolarisQ MS and Mr Clive Dixon for design and fabrication of the high vacuum vaporization + condensation glassware.

## 7. References

1. V. I. Parvulescu and C. Hardacre, *Chem. Rev.*, 2007, **107**, 2615-2665.
2. M. Armand, F. Endres, D. R. MacFarlane, H. Ohno and B. Scrosati, *Nat. Mater.*, 2009, **8**, 621-629.
3. C. F. Poole and S. K. Poole, *J. Sep. Sci.*, 2011, **34**, 888-900.
4. F. Zhou, Y. M. Liang and W. M. Liu, *Chem. Soc. Rev.*, 2009, **38**, 2590-2599.
5. A. Brandt, J. Gräsvik, J. P. Hallett and T. Welton, *Green Chem.*, 2013, **15**, 550-583.
6. Y. F. Hu, Z. C. Liu, C. M. Xu and X. M. Zhang, *Chem. Soc. Rev.*, 2011, **40**, 3802-3823.
7. C. Tian, W. L. Nie, Q. Chen, G. F. Sun, J. P. Hu and M. V. Borzov, *Russ. Chem. Bull.*, 2014, **63**, 2668-2674.
8. K. Chansaenpak, M. Z. Wang, Z. H. Wu, R. Zaman, Z. B. Li and F. P. Gabbai, *Chem. Commun.*, 2015, **51**, 12439-12442.
9. B. Vabre, K. Chansaenpak, M. Z. Wang, H. Wang, Z. B. Li and F. P. Gabbai, *Chem. Commun.*, 2017, **53**, 8657-8659.
10. K. Chansaenpak, M. Z. Wang, H. Wang, B. C. Giglio, F. P. Gabba, Z. H. Wu and Z. B. Li, *Rsc Advances*, 2017, **7**, 17748-17751.
11. T. Bottcher and G. V. Roschenthaler, *J. Fluor. Chem.*, 2015, **171**, 4-11.
12. C. Maton, N. De Vos and C. V. Stevens, *Chem. Soc. Rev.*, 2013, **42**, 5963-5977.
13. H. L. Ngo, K. LeCompte, L. Hargens and A. B. McEwen, *Thermochim. Acta*, 2000, **357**, 97-102.
14. C. P. Fredlake, J. M. Crosthwaite, D. G. Hert, S. Aki and J. F. Brennecke, *J. Chem. Eng. Data*, 2004, **49**, 954-964.
15. W. H. Awad, J. W. Gilman, M. Nyden, R. H. Harris, T. E. Sutto, J. Callahan, P. C. Trulove, H. C. DeLong and D. M. Fox, *Thermochim. Acta*, 2004, **409**, 3-11.
16. J. G. Huddleston, A. E. Visser, W. M. Reichert, H. D. Willauer, G. A. Broker and R. D. Rogers, *Green Chem.*, 2001, **3**, 156-164.
17. D. H. Zaitsau, Y. U. Paulechka and G. J. Kabo, *J. Phys. Chem. A*, 2006, **110**, 11602-11604.
18. B. K. M. Chan, N. H. Chang and M. R. Grimmett, *Aust. J. Chem.*, 1977, **30**, 2005-2013.
19. H. Ohtani, S. Ishimura and M. Kumai, *Anal. Sci.*, 2008, **24**, 1335-1340.
20. N. Meine, F. Benedito and R. Rinaldi, *Green Chem.*, 2010, **12**, 1711-1714.
21. Y. Hao, J. Peng, S. W. Hu, J. G. Li and M. L. Zhai, *Thermochim. Acta*, 2010, **501**, 78-83.
22. K. R. J. Lovelock, J. P. Armstrong, P. Licence and R. G. Jones, *Phys. Chem. Chem. Phys.*, 2014, **16**, 1339-1353.
23. S. D. Chambreau, J. A. Boatz, G. L. Vaghjiani, C. Koh, O. Kostko, A. Golan and S. R. Leone, *J. Phys. Chem. A*, 2012, **116**, 5867-5876.
24. S. D. Chambreau, A. C. Schenk, A. J. Sheppard, G. R. Yandek, G. L. Vaghjiani, J. Maciejewski, C. J. Koh, A. Golan and S. R. Leone, *J. Phys. Chem. A*, 2014, **118**, 11119-11132.
25. J. B. Liu, S. D. Chambreau and G. L. Vaghjiani, *J. Phys. Chem. A*, 2014, **118**, 11133-11144.
26. M. T. Clough, K. Geyer, P. A. Hunt, J. Mertes and T. Welton, *Phys. Chem. Chem. Phys.*, 2013, **15**, 20480-20495.
27. V. Volpe, B. Brunetti, G. Gigli, A. Lapi, S. V. Cipriotti and A. Ciccioli, *J. Phys. Chem. B*, 2017, **121**, 10382-10393.

28. A. W. Taylor, K. R. J. Lovelock, R. G. Jones and P. Licence, *Dalton Trans.*, 2011, **40**, 1463-1470.
29. C. Tian, W. L. Nie, M. V. Borzov and P. F. Su, *Organometallics*, 2012, **31**, 1751-1760.
30. M. C. Kroon, W. Buijs, C. J. Peters and G. J. Witkamp, *Thermochim. Acta*, 2007, **465**, 40-47.
31. P. Ballone and R. Cortes-Huerto, *Faraday Discuss.*, 2012, **154**, 373-389.
32. M. J. Earle, J. M. S. S. Esperança, M. A. Gilea, J. N. Canongia Lopes, L. P. N. Rebelo, J. W. Magee, K. R. Seddon and J. A. Widegren, *Nature*, 2006, **439**, 831-834.
33. K. R. J. Lovelock, *R. Soc. Open Sci.*, 2017, **4**, 171223.
34. J. P. Armstrong, C. Hurst, R. G. Jones, P. Licence, K. R. J. Lovelock, C. J. Satterley and I. J. Villar-Garcia, *Phys. Chem. Chem. Phys.*, 2007, **9**, 982-990.
35. V. N. Emel'yanenko, S. P. Verevkin, A. Heintz, J. A. Corfield, A. Deyko, K. R. J. Lovelock, P. Licence and R. G. Jones, *J. Phys. Chem. B*, 2008, **112**, 11734-11742.
36. A. Deyko, K. R. J. Lovelock, J. A. Corfield, A. W. Taylor, P. N. Gooden, I. J. Villar-Garcia, P. Licence, R. G. Jones, V. G. Krasovskiy, E. A. Chernikova and L. M. Kustov, *Phys. Chem. Chem. Phys.*, 2009, **11**, 8544-8555.
37. K. R. J. Lovelock, A. Deyko, P. Licence and R. G. Jones, *Phys. Chem. Chem. Phys.*, 2010, **12**, 8893-8901.
38. A. W. Taylor, K. R. J. Lovelock, A. Deyko, P. Licence and R. G. Jones, *Phys. Chem. Chem. Phys.*, 2010, **12**, 1772-1783.
39. A. Deyko, K. R. J. Lovelock, P. Licence and R. G. Jones, *Phys. Chem. Chem. Phys.*, 2011, **13**, 16841-16850.
40. A. Deyko, S. G. Hessey, P. Licence, E. A. Chernikova, V. G. Krasovskiy, L. M. Kustov and R. G. Jones, *Phys. Chem. Chem. Phys.*, 2012, **14**, 3181-3193.
41. S. G. Hessey and R. G. Jones, *Chem. Sci.*, 2013, **4**, 2519-2529.
42. J. P. Leal, J. M. S. S. Esperança, M. E. M. da Piedade, J. N. Canongia Lopes, L. P. N. Rebelo and K. R. Seddon, *J. Phys. Chem. A*, 2007, **111**, 6176-6182.
43. J. H. Gross, *J. Am. Soc. Mass Spectrom.*, 2008, **19**, 1347-1352.
44. D. Strasser, F. Goulay, M. S. Kelkar, E. J. Maginn and S. R. Leone, *J. Phys. Chem. A*, 2007, **111**, 3191-3195.
45. S. D. Chambreau, G. L. Vaghjiani, A. To, C. Koh, D. Strasser, O. Kostko and S. R. Leone, *J. Phys. Chem. B*, 2010, **114**, 1361-1367.
46. D. Strasser, F. Goulay, L. Belau, O. Kostko, C. Koh, S. D. Chambreau, G. L. Vaghjiani, M. Ahmed and S. R. Leone, *J. Phys. Chem. A*, 2010, **114**, 879-883.
47. S. D. Chambreau, G. L. Vaghjiani, C. J. Koh, A. Golan and S. R. Leone, *J. Phys. Chem. Lett.*, 2012, **3**, 2910-2914.
48. C. J. Koh and S. R. Leone, *Mol. Phys.*, 2012, **110**, 1705-1712.
49. E. I. Obi, C. M. Leavitt, P. L. Raston, C. P. Moradi, S. D. Flynn, G. L. Vaghjiani, J. A. Boatz, S. D. Chambreau and G. E. Douberly, *J. Phys. Chem. A*, 2013, **117**, 9047-9056.
50. R. Cooper, A. M. Zolot, J. A. Boatz, D. P. Sporleder and J. A. Stearns, *J. Phys. Chem. A*, 2013, **117**, 12419-12428.
51. N. S. Chilingarov, A. A. Medvedev, G. S. Deyko, L. M. Kustov, E. A. Chernikova, L. M. Glukhov, V. Y. Markov, I. Y. N. Ioffe, V. M. Senyavin, M. V. Polyakova and L. N. Sidorov, *Rapid Commun. Mass Spectrom.*, 2015, **29**, 1227-1232.
52. A. M. Dunaev, V. B. Motalov, L. S. Kudin and M. F. Butman, *J. Mol. Liq.*, 2016, **219**, 599-601.
53. A. M. Dunaev, V. B. Motalov, L. S. Kudin and M. F. Butman, *J. Mol. Liq.*, 2016, **223**, 407-411.
54. A. Tolstogouzov, U. Bardi, O. Nishikawa and M. Taniguchi, *Surf. Interface Anal.*, 2008, **40**, 1614-1618.
55. B. Brunetti, A. Ciccioli, G. Gigli, A. Lapi, N. Misceo, L. Tanzi and S. V. Cipriotti, *Phys. Chem. Chem. Phys.*, 2014, **16**, 15653-15661.
56. M. S. Kelkar and E. J. Maginn, *J. Phys. Chem. B*, 2007, **111**, 9424-9427.
57. N. Rai and E. J. Maginn, *Faraday Discuss.*, 2012, **154**, 53-69.
58. P. Ballone, C. Pinilla, J. Kohanoff and M. G. Del Pópolo, *J. Phys. Chem. B*, 2007, **111**, 4938-4950.



59. V. V. Chaban and O. V. Prezhdo, *J. Phys. Chem. Lett.*, 2012, **3**, 1657-1662.
60. D. H. Zaitsau, A. V. Yermalaye, V. N. Emel'yanenko, S. Butler, T. Schubert and S. P. Verevkin, *J. Phys. Chem. B*, 2016, **120**, 7949-7957.
61. D. H. Zaitsau, A. V. Yermalaye, T. J. S. Schubert and S. P. Verevkin, *J. Mol. Liq.*, 2017, **242**, 951-957.
62. A. Seeberger, A. K. Andresen and A. Jess, *Phys. Chem. Chem. Phys.*, 2009, **11**, 9375-9381.
63. F. Heym, B. J. M. Etzold, C. Kern and A. Jess, *Phys. Chem. Chem. Phys.*, 2010, **12**, 12089-12100.
64. F. Heym, B. J. M. Etzold, C. Kern and A. Jess, *Green Chem.*, 2011, **13**, 1453-1466.
65. F. Heym, W. Korth, J. Thiessen, C. Kern and A. Jess, *Chem. Ing. Tech.*, 2015, **87**, 791-802.
66. D. H. Zaitsau, K. Fumino, V. N. Emel'yanenko, A. V. Yermalaye, R. Ludwig and S. P. Verevkin, *ChemPhysChem*, 2012, **13**, 1868-1876.
67. M. G. Freire, C. M. S. S. Neves, I. M. Marrucho, J. A. P. Coutinho and A. M. Fernandes, *J. Phys. Chem. A*, 2010, **114**, 3744-3749.
68. K. R. J. Lovelock, E. F. Smith, A. Deyko, I. J. Villar-Garcia, P. Licence and R. G. Jones, *Chem. Commun.*, 2007, 4866-4868.
69. K. R. J. Lovelock, A. Deyko, J. A. Corfield, P. N. Gooden, P. Licence and R. G. Jones, *ChemPhysChem*, 2009, **10**, 337-340.
70. S. P. Verevkin, D. H. Zaitsau, V. N. Emelyanenko and A. Heintz, *J. Phys. Chem. B*, 2011, **115**, 12889-12895.
71. D. H. Zaitsau, S. P. Verevkin, V. N. Emel'yanenko and A. Heintz, *ChemPhysChem*, 2011, **12**, 3609-3613.
72. K. Fumino, T. Peppel, M. Geppert-Rybczynska, D. H. Zaitsau, J. K. Lehmann, S. P. Verevkin, M. Köckerling and R. Ludwig, *Phys. Chem. Chem. Phys.*, 2011, **13**, 14064-14075.
73. V. N. Emel'yanenko, D. H. Zaitsau, S. P. Verevkin, A. Heintz, K. Voss and A. Schulz, *J. Phys. Chem. B*, 2011, **115**, 11712-11717.
74. D. H. Zaitsau, A. V. Yermalaye, V. N. Emel'yanenko, S. P. Verevkin, U. Welz-Biermann and T. Schubert, *Sci. China-Chem.*, 2012, **55**, 1525-1531.
75. S. P. Verevkin, D. H. Zaitsau, V. N. Emel'yanenko, R. V. Ralys, A. V. Yermalaye and C. Schick, *J. Chem. Thermodyn.*, 2012, **54**, 433-437.
76. S. P. Verevkin, D. H. Zaitsau, V. N. Emel'yanenko, A. V. Yermalaye, C. Schick, H. J. Liu, E. J. Maginn, S. Bulut, I. Krossing and R. Kalb, *J. Phys. Chem. B*, 2013, **117**, 6473-6486.
77. D. H. Zaitsau, A. V. Yermalaye, V. N. Emel'yanenko, C. Schick, S. P. Verevkin, A. A. Samarov, S. Schlenk and P. Wasserscheid, *Z. Phys. Chemie-Int. J. Res. Phys. Chem. Chem. Phys.*, 2013, **227**, 205-215.
78. D. H. Zaitsau, A. V. Yermalaye, S. P. Verevkin, J. E. Bara and A. D. Stanton, *Ind. Eng. Chem. Res.*, 2013, **52**, 16615-16621.
79. D. H. Zaitsau, A. V. Yermalaye, V. N. Emel'yanenko, A. Heintz, S. P. Verevkin, C. Schick, S. Berdzinski and V. Strehmel, *J. Mol. Liq.*, 2014, **192**, 171-176.
80. D. H. Zaitsau, A. V. Yermalaye, S. P. Verevkin, J. E. Bara and D. A. Wallace, *Thermochim. Acta*, 2015, **622**, 38-43.
81. D. H. Zaitsau, M. A. Varfolomeev, S. P. Verevkin, A. D. Stanton, M. S. Hindman and J. E. Bara, *J. Chem. Thermodyn.*, 2016, **93**, 151-156.
82. D. H. Zaitsau, M. Kaliner, S. Lerch, T. Strassner, V. N. Emel'yanenko and S. P. Verevkin, *Z. Anorg. Allg. Chem.*, 2017, **643**, 114-119.
83. D. H. Zaitsau, A. V. Yermalaye, V. N. Emel'yanenko, A. Schulz and S. P. Verevkin, *Z. Anorg. Allg. Chem.*, 2017, **643**, 87-92.
84. A. V. Yermalaye, D. H. Zaitsau, M. Loor, J. Schaumann, V. N. Emel'yanenko, S. Schulz and S. P. Verevkin, *Z. Anorg. Allg. Chem.*, 2017, **643**, 81-86.
85. A. V. Yermalaye, D. H. Zaitsau, V. N. Emel'yanenko and S. P. Verevkin, *J. Solut. Chem.*, 2015, **44**, 754-768.

86. Y. U. Paulechka, D. H. Zaitsau, G. J. Kabo and A. A. Strechan, *Thermochim. Acta*, 2005, **439**, 158-160.
87. D. H. Zaitsau, G. J. Kabo, A. A. Strechan, Y. U. Paulechka, A. Tschersich, S. P. Verevkin and A. Heintz, *J. Phys. Chem. A*, 2006, **110**, 7303-7306.
88. E. Paulechka, A. V. Blokhin, A. S. M. C. Rodrigues, M. A. A. Rocha and L. M. N. B. F. Santos, *J. Chem. Thermodyn.*, 2016, **97**, 331-340.
89. M. A. A. Rocha, C. F. R. A. C. Lima, L. R. Gomes, B. Schröder, J. A. P. Coutinho, I. M. Marrucho, J. M. S. S. Esperança, L. P. N. Rebelo, K. Shimizu, J. N. Canongia Lopes and L. M. N. B. F. Santos, *J. Phys. Chem. B*, 2011, **115**, 10919-10926.
90. M. A. A. Rocha, J. A. P. Coutinho and L. M. N. B. F. Santos, *J. Phys. Chem. B*, 2012, **116**, 10922-10927.
91. M. A. A. Rocha and L. M. N. B. F. Santos, *Chem. Phys. Lett.*, 2013, **585**, 59-62.
92. M. A. A. Rocha, J. A. P. Coutinho and L. M. N. B. F. Santos, *J. Chem. Phys.*, 2014, **141**, 8.
93. M. A. A. Rocha, F. M. S. Ribeiro, B. Schröder, J. A. P. Coutinho and L. M. N. B. F. Santos, *J. Chem. Thermodyn.*, 2014, **68**, 317-321.
94. A. S. M. C. Rodrigues, C. F. R. A. C. Lima, J. A. P. Coutinho and L. M. N. B. F. Santos, *Phys. Chem. Chem. Phys.*, 2017, **19**, 5326-5332.

